SANDIA REPORT
SAND2020-2378
Printed February 2020

Sandia National Laboratories

Antenna Requirements for GMTI Radar Systems

Armin W Doerry, Douglas L Bickel

Prepared by
Sandia National Laboratories
Albuquerque, New Mexico
87185 and Livermore,
California 94550

Issued by Sandia National Laboratories, operated for the United States Department of Energy by National Technology & Engineering Solutions of Sandia, LLC.

Available to DOE and DOE contractors from
U.S. Department of Energy
Office of Scientific and Technical Information
P.O. Box 62
Oak Ridge, TN 37831

Telephone: (865) 576-8401
Facsimile: (865) 576-5728
E-Mail: reports@osti.gov
Online ordering: http://www.osti.gov/scitech

Available to the public from
U.S. Department of Commerce
National Technical Information Service
5301 Shawnee Rd
Alexandria, VA 22312

Telephone: (800) 553-6847
Facsimile: (703) 605-6900
E-Mail: orders@ntis.gov
Online order: https://classic.ntis.gov/help/order-methods/

Abstract

A principal performance-enabling, or performance-limiting, component of Ground-Moving-Target-Indication (GMTI) radar systems is the antenna. Undesired clutter leakage into antenna sidelobes can be particularly problematic, generating undesired false alarms. GMTI system antennas can be designed with characteristics and features to allow discriminating and depressing/suppressing problematic sidelobe leakage of clutter and other undesired signals. We offer analysis and design guidelines for doing so.

Acknowledgements

This report was funded by General Atomics Aeronautical Systems, Inc. (GA-ASI) Mission Systems under Cooperative Research and Development Agreement (CRADA) SC08/01749 between Sandia National Laboratories and GA-ASI.

General Atomics Aeronautical Systems, Inc. (GA-ASI), an affiliate of privately-held General Atomics, is a leading manufacturer of Remotely Piloted Aircraft (RPA) systems, radars, and electro-optic and related mission systems, including the Predator®/Gray Eagle®-series and Lynx® Multi-mode Radar.

Contents

List of Figures

List of Tables

Acronyms and Definitions

1-D, 2-D, 3-D	1-, 2-, 3-Dimesional
AESA	Active Electronically Steered Array
AWGN	Additive White Gaussian Noise
ATI	Along-Track Interferometry
CCD	Coherent Change Detection
CPI	Coherent Processing Interval
CNR	Clutter to Noise Ratio
DMTI	Dismount Moving Target Indicator
DOA	Direction of Arrival
DPCA	Displaced Phase Center Antenna
EM	Electromagnetic
ESA	Electronically Steered Array
FAM	False Alarm Mitigation
FAR	False Alarm Rate
GMTI	Ground Moving Target Indicator
HRR	High Range Resolution
ICM	Internal Clutter Motion
IPR	Impulse Response
MDV	Minimum Detectable Velocity
MTI	Moving Target Indicator
PRF	Pulse Repetition Frequency
RCS	Radar Cross Section
RX	Receive or Receiver
SAR	Synthetic Aperture Radar
SCR	Signal to Clutter Ratio
SINR	Signal to Interference plus Noise
SLB	Sidelobe Blanking
SLC	Sidelobe Cancellation
SNR	Signal to Noise Ratio
STAP	Space-Time Adaptive Processing
TX	Transmit or Transmitter

Foreword

This report details the results of an academic study. It does not presently exemplify any modes, methodologies, or techniques employed by any operational system known to the authors.

Classification

The specific mathematics and algorithms presented herein do not bear any release restrictions or distribution limitations.

This report formalizes preexisting informal notes and other documentation on the subject matter herein.

Author Contact Information

Armin Doerry	awdoerr@sandia.gov	505-845-8165
Doug Bickel	dlbicke@sandia.gov	505-845-9038

1 Introduction and Background

There is perhaps no more important circuit element than the antenna for setting the performance limits in a radar system. This is especially true for Ground Moving Target Indicator (GMTI) radar systems, a class of Moving Target Indicator (MTI) radars intended to detect and locate land-based moving targets. For GMTI systems, the nature of the antenna beam, or beams for multi-aperture/beam antennas, defines limits on the detectability of targets of interest in the presence of clutter and other interference.

One aspect of antenna beam shape that influences GMTI capabilities is the overall antenna aperture illumination, which defines the sidelobe structure of the beam. Antenna sidelobes allow energy to be collected from otherwise undesirable directions, often providing interference to the desired operation of the radar system.

Our interest for this report is primarily microwave GMTI radar systems. Some antenna technologies, such as parabolic dish reflector antennas, provide some degree of natural aperture tapering with attendant "nice" sidelobe reductions. However, the advent of multi-aperture or multi-beam antennas, especially more than two, favor array antenna architectures. These might still be corporate-fed antennas, or they might be distributed-power-amplifier antennas. They might be Electronically Steered Array (ESA) antennas, or Active Electronically Steered Array (AESA) antennas. Such antennas do not favor aperture tapering, favoring uniform aperture illumination, as tapering often implies an undesirable loss in transmitted power.

So, as a GMTI radar system designer, we are left with questions that must be answered to make proper feature selection and performance trades. These include

1. What exactly should be antenna beam pattern requirements for the antenna?
2. How do antenna sidelobes impact GMTI operation and performance?
3. What can we do to overcome undesired antenna sidelobe effects?
4. What antenna design features benefit GMTI operation and performance?

We offer as general references to provide background for this report the following source.

> The Sandia Report SAND2010-5844 provides a discussion of general performance issues for GMTI radar systems.[1]

“If you've heard this story before, don't stop me, because I'd like to hear it again.”
-- Groucho Marx

2 GMTI Radar Echoes

Processing GMTI radar data requires us to contend with four main classes of echo energy. These are

1. Moving discrete reflector targets
2. Distributed ground clutter
3. Discrete ground clutter
4. Interfering signals
5. System noise, presumed to be Additive White Gaussian Noise (AWGN)

Of these, for GMTI radar systems, we are typically interested only in the first. The other classes confuse our ability to detect and locate targets of interest. Clutter and interfering signals are often referred to collectively as "interference." Consequently, a measure of desirable target echo quality is typically the Signal-to-Interference-plus-Noise-Ratio (SINR). The absolute measure of reflection strength is Radar Cross Section (RCS). These measures and ratios are in terms of power/energy, often expressed in logarithmic units of dB.

We now examine these various classes in turn.

2.1 Moving Targets

The targets of interest for GMTI systems generally can be divided into two classes.

1. The first is ground vehicles, i.e. automobiles, trucks, military armored vehicles, etc. A subset of ground vehicles might include motorcycles and/or bicycles.
2. The second is people, often termed "dismounts." GMTI systems designed or operated to detect/locate dismounts are often called Dismount Moving Target Indicator (DMTI) radars.

Maritime MTI targets are not specifically included in the discussion of this report, although much in this report might still be applicable. Also not included are Airborne MTI targets, with the possible exception of low-flying slow aircraft such as smaller unmanned systems/drones, ultralight aircraft, etc. These low/slow targets can be termed "near-ground" targets.

2.1.1 Ground Vehicles

Vehicle RCS statistics can be found throughout the literature, with Raynal, et al.,[2] providing an excellent discussion and reference list for X-band and Ku-band microwave frequencies.

A very typical requirement is to detect a +10 dBsm vehicle, exemplified by perhaps a pickup truck. We do note that a vehicles RCS is very aspect dependent, with statistics over aspect angle suggesting that a vehicle with average RCS of +10 dBsm will be above 0 dBsm over about 90%

of aspect angles. Consequently, for 90% of aspect angles, a detection threshold reasonably should be no higher than 0 dBsm.

Motorcycles and bicycles will exhibit RCS somewhat less than automobiles and trucks, but more than dismounts.

2.1.2 Dismounts

Dismount RCS statistics are somewhat less plentiful in the literature. Raynal, et al.,[3] also provide an excellent discussion and reference list for dismount RCS statistics at Ku-band.

Minimum requirements for DMTI operation are suggested in a paper by Doerry, et al.[4] This includes the recommendation that a detection threshold should be no higher than −10 dBsm. In addition, maximum dismount velocities tend to be not much greater than about 2 m/s or so.

2.2 Distributed Ground Clutter

Distributed ground clutter is the natural terrain illuminated by the radar, with RCS dependent on resolved area. Consequently, it is measured in units normalized to some area, usual 1 m^2. Typical quantities for various terrain types are given in books by Long,[5] and by Ulaby and Dobson.[6] Distributed clutter typically exhibits a Rayleigh-distributed magnitude, and a Uniform random phase. Reflectivity values are usually a statistical measure, such as an average.

Clutter reflectivity values are frequency/wavelength dependent, and grazing angle dependent. A typical upper value for clutter reflectivity at Ku-band for natural clutter might be on the order of −10 dBsm/ m^2, equating to 0.1 m^2/m^2. The RCS of a resolution cell containing distributed ground clutter may be calculated as

$$\sigma_{clutter} = \frac{\rho_r \rho_a \sigma_0}{\cos\psi}, \tag{1}$$

where

σ_0 = normalized clutter reflectivity with units m^2/m^2,
ρ_r = slant-range resolution of the radar with units m,
ρ_a = azimuth (cross-range) resolution of the radar with units m, and
ψ = local grazing angle. (2)

The azimuth resolution of the radar may be calculated as the lesser due to antenna azimuth beamwidth, and that due to a corresponding Doppler resolution,

$$\rho_a = \min\left(\frac{a_{w,d} \lambda R}{2 v_\perp T_{CPI}}, \Theta \right), \tag{3}$$

where

λ = nominal wavelength of the radar signal with units m,
R = nominal operating slant-range with units m,
$v_{\perp}$ = cross-range velocity component in units of m/s,
T_{CPI} = Coherent Processing Interval (CPI) duration in units of s,
$a_{w,d}$ = Doppler Impulse Response (IPR) broadening factor due to data tapering, and
Θ = nominal antenna azimuth beamwidth. (4)

The parameter $a_{w,d}$ depends on the window taper function employed in Doppler processing.[7]

Example

Consider a Ku-band GMTI radar operating with 18 mm wavelength, at 10 km range, 100 m/s cross-range velocity, 0.1 s CPI length, processed with data Doppler tapering factor $a_{w,d} = 1.2$. This yields an azimuth resolution of 10.8 m.

Now further assume a clutter reflectivity of -10 dBsm/ m^2, 10 m range resolution, and a nominal 20 deg. grazing angle. This yields an RCS for a clutter cell of 11.5 m^2, or 10.6 dBsm. Note that this increases with longer range or slower radar velocity.

2.3 Discrete Ground Clutter

Clutter, both natural and cultural (man-made), is usually not uniform (homogeneous), and typically also exhibits spatially-random specular or discrete reflections, often called "clutter discretes." While more prevalent in cultural scenes, they do in fact also exist in natural settings.

Cultural clutter was characterized at Ku-band in a paper by Raynal, et al.[8] She notes that a scene containing typically some cultural features will contain clutter discretes that exceed +45 dBsm approximately once per square mile.

Stralka and Fedarke, in Skolnik's Radar Handbook,[9] offer a model for the density of clutter discretes at "higher radar frequencies" given in the following table.

Table 1. Discrete Clutter Density

RCS	*Density (per sq. mile)*
10^6 m^2 (60 dBsm)	0.01
10^5 m^2 (50 dBsm)	0.1
10^4 m^2 (40 dBsm)	1

The bottom line is that strong clutter discretes are relatively sparse, but they do exist. We also acknowledge that stationary ground clutter may not always be perfectly stationary, and may exhibit some small range of velocity due to, for example, wind-driven motion. This is often called "Internal Clutter Motion" (ICM).

2.4 Interfering Signals

Interfering Signals for this report are energy that is other than clutter echoes, or broadband system noise. This might include jamming (either intentional or not) or spoofing.

For this report, it will be presumed that these signals will be controlled through design and/or signal processing so that we will not need to consider them further.

2.5 System Noise

System noise for this report is the broadband, assumed AWGN, noise floor to the radar data resulting from natural radiated emissions from the target scene, along with internally (to the radar) generated noise. The Sandia Report SAND2016-9649 offers a detailed discussion of noise in radar receivers.[10]

The ability to detect targets with limited false alarms is highly dependent on the level of system noise in the data, especially after any signal processing. We note that coherent processing of data will increase the Signal-to-Noise Ratio (SNR), aiding the detection process. Typical GMTI processing involves generating a range-Doppler map that is then input to a detection algorithm.

A basic discussion of detection theory is given in an appendix of Sandia Report SAND2010-5844.[1] Generally, for a fixed SNR, improving the Probability of Detection (P_D) comes at the expense of an increased False Alarm Rate (FAR). The only way to increase P_D without increasing FAR, is to increase the SNR.

Typically, acceptable detection performance is often had with an SNR of about 15 dB in the final range-Doppler image, although good Direction of Arrival (DOA) measurements may require more. Noting that clutter mitigation techniques will generally diminish SNR somewhat for Doppler regions of interest. Consequently, an SNR of perhaps 20 dB absent any clutter mitigation, and in fact ignoring clutter, is perhaps a better minimum operating point. Clutter mitigation effects on SNR is discussed in a paper by Bickel and Doerry.[11]

Consequently, the recommended system noise level is perhaps no higher than 20 dB below the minimum threshold target RCS level.

2.6 Comments

It is our desire to detect legitimate targets and nothing else. We have noted that detection theory suggests that we desire any broadband system noise to manifest no higher than 20 dB below the minimum target RCS we wish to detect.

Clutter, however, whether distributed or discrete, can offer RCS that is comparable, or even substantially exceeds, the RCS of desired legitimate targets. Consequently, only if clutter can be suppressed or mitigated to below the detection level, can the clutter be rendered to not cause any false alarms. If it can be rendered to below the maximum allowable noise level, then it will not impact the detection process at all.

Example

> Consider that we wish to detect dismounts down to an RCS of −10 dBsm, in the presence of discrete clutter with RCS of +45 dBsm. This means that the discrete clutter will need to be suppressed by 55 dB so as not to generate a false alarm. If we wish to not affect the detection process at all, then it will need to be suppressed by perhaps 65 dB or more.

“Those are my principles, and if you don't like them... well, I have others.”
-- Groucho Marx

3 Uniform Aperture Characteristics

We now consider a simple single-phase-center, single-beam, monostatic, perfectly efficient, uniformly-illuminated aperture antenna. For simplicity, we consider a 2-Dimensional (2-D) geometry.

We define its aperture illumination function as

$$x(l) = \text{rect}\left(\frac{l}{L}\right), \tag{5}$$

where

L = the length of the aperture with units m, and

$$\text{rect}(z) = \begin{cases} 1 & |z| \le 0.5 \\ 0 & else \end{cases}. \tag{6}$$

The far-field pattern of this aperture illumination is

$$X(\theta) = L\,\text{sinc}\left(\frac{\sin\theta}{\lambda/L}\right), \tag{7}$$

where

θ = DOA angle with respect to broadside with units of radians, and

$$\text{sinc}(z) = \frac{\sin(\pi z)}{\pi z}. \tag{8}$$

Eq. (7) describes the one-way antenna pattern in terms of field strength of a transmitted or radiated signal. The one-way radiated power is the square of this.

We observe that the nominal width of the mainlobe is the conventional equation

$$\Theta \approx \lambda/L \text{ = nominal beamwidth,} \tag{9}$$

and the null-to-null beamwidth is twice this. We further note that this is most accurate for $L \gg \lambda$.

We are assuming a monostatic radar operation, where the receive antenna is the same as the transmit antenna. We will assume no modification of the antenna characteristics between transmit and receive. Consequently, the two-way antenna pattern is the transmit pattern multiplied by the identical receive pattern. For monostatic radar, it is the two-way pattern that ultimately counts. For the uniformly-illuminated aperture antenna, we plot the two-way pattern in Figure 1.

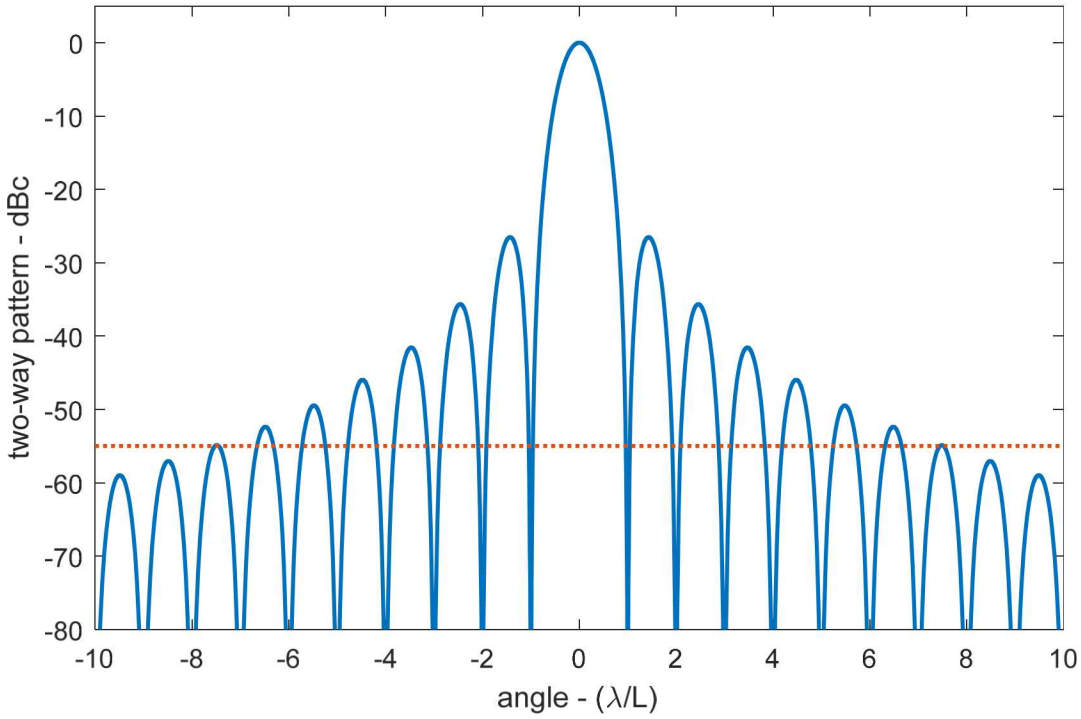

Figure 1. Two-way antenna pattern for uniform aperture.

We now illustrate the issue of this report with the following example.

Example

Consider a dismount target in the direction of the beam center with RCS of −10 dBsm. Now also consider a +45 dBsm clutter discrete located at 4.5 nominal beamwidths from the beam center. This is well outside of the mainlobe, but in an antenna pattern sidelobe. The attenuation here is about −46 dB, meaning the clutter discrete will "leak" through at a level of −1 dBsm, well above the dismount's response. If our detection threshold is −10 dBsm, then the clutter discrete will generate a false alarm, absent any other mitigation schemes. In fact, this clutter discrete would need to be beyond about 7.5 beamwidths to be attenuated sufficiently to not cause a false alarm.

We also note that had the clutter discrete appeared at an angle where the antenna pattern exhibits a null, then it would be completely attenuated and be no competition at all for the dismount target.

In any case, any clutter with RCS below +16 dBsm will not pass the −10 dBsm detection threshold if observed through any sidelobe. It may still be detectable in the mainlobe.

We take from all this that for clutter to not cause a false alarm, it needs to be attenuated to below the detection threshold, not only in the mainlobe of the antenna, but also in the sidelobes. We stipulate that at Ku-band, this attenuation needs to be about −55 dB for DMTI, but can probably be relaxed to −45 dB for vehicles.

4 Relating Angle to Doppler and Velocity

GMTI radar is usually implemented by measuring target closing velocity via Doppler shift, with Doppler shift measured as a pulse-to-pulse time-delay or phase shift. Problematic for us is that even stationary clutter will exhibit a closing velocity, in fact a spectrum of velocities.

Consider the linear aperture of the previous section aligned with the radar's direction of travel.

The moving aperture will exhibit a line-of-sight velocity component in the direction θ calculated as

$$v_{los}(\theta) = v_a \sin\theta, \tag{10}$$

where

v_a = the forward velocity of the radar in the direction of travel. (11)

We are tacitly assuming that the antenna beam boresight is pointed at zero-Doppler, and a positive angle θ is always forward of broadside.

The line-of-sight velocity of Eq. (10) will cause a stationary target to exhibit a Doppler shift of

$$f_d(\theta) = \frac{2}{\lambda} v_{los}(\theta) = \frac{2v_a}{\lambda} \sin\theta. \tag{12}$$

We note that directions forward of broadside will cause a positive Doppler shift for stationary targets, and directions aft of broadside will cause a negative Doppler shift.

For small angles, Eq. (12) may be approximated as the linear relationship

$$f_d(\theta) \approx \frac{2v_a}{\lambda} \theta. \tag{13}$$

We illustrate these relationships with the following examples.

Example

Consider the antenna and example of the previous section. We now calculate under what conditions we can detect a 1 m/s dismount line-of-sight velocity without any false alarms from a +45 dBsm clutter discrete.

We force the correspondence of 7.5 beamwidths to 1 m/s line-of-sight velocity, using Eq. (10). This yields

$$1 = v_a \sin(7.5\,\lambda/L) \approx \frac{7.5\,\lambda v_a}{L}. \tag{14}$$

For a Ku-band radar with 18 mm wavelength, this becomes the condition

$$\frac{L}{v_a} \approx 0.135 . \tag{15}$$

Candidate design points include an aircraft velocity of 7.4 m/s for a 1 m aperture, or a 13.5 m aperture at 100 m/s. Both of these are problematic for most practical aircraft.

Example

Now consider a Ku-band GMTI radar with uniformly illuminated aperture designed to detect vehicles with a threshold of 0 dBsm, and minimum velocity of 2 m/s. Consider also that we are concerned only with clutter discretes of +35 dBsm, having a mitigation scheme for false alarms from larger clutter discretes.

Consequently, we require –35 dB of clutter attenuation in sidelobes, which corresponds to about 1.74 beamwidths from the center of the mainlobe. For a Ku-band radar with 18 mm wavelength, this becomes the condition

$$\frac{L}{v_a} \approx 0.0157 . \tag{16}$$

Candidate design points include an aircraft velocity of 63.8 m/s for a 1 m aperture, or a 1.57 m aperture at 100 m/s. Both of these are quite reasonable for many practical aircraft.

5 Tapered Aperture Characteristics

Previous sections dealt with uniformly illuminated apertures. We now allow aperture tapering for sidelobe control. The literature contains many articles discussing various taper functions and their characteristics and utility. Sandia Report SAND2017-4042 catalogs a number of these.[12]

We will arbitrarily choose a Hamming window taper function to be representative of the utility of aperture tapering. We note that the Hamming window comes with a 1.35 dB relative SNR loss for each aperture, transmit and receive.

We first consider an antenna with the Hamming taper for both transmit and receive antennas. The two-way pattern is illustrated in Figure 2. We note that although the mainlobe is broader, having width of $1.3\lambda/L$ at the −6 dBc points, all sidelobes are well below a −10 dBsm detection threshold for a +45 dBsm clutter discrete.

We now consider an antenna with a Hamming taper on transmit only, and a uniform taper on receive. The two-way pattern for this is illustrated in Figure 3. We note that the mainlobe has narrowed from that of Figure 2, now having width of $1.025\lambda/L$ at the −6 dBc points. However, the narrower mainlobe has also split to manifest two sidelobes, each peaking at about −27 dBc. With a −10 dBsm detection threshold, any clutter discrete greater than +17 dBsm risks being detected via the sidelobe.

Example

Consider a Ku-band DMTI radar with the two-way antenna pattern of Figure 2. From Figure 2 we observe that the response to a +45 dBsm clutter discrete falls below our −10 dBsm detection threshold at an angle offset of $1.715\lambda/L$. If we force this angle to correspond to 1 m/s, then we constrain

$$\frac{L}{v_a} \approx 0.0309. \tag{17}$$

Candidate design points include an aircraft velocity of 32.4 m/s for a 1 m aperture, or a 3.09 m aperture at 100 m/s. These are not entirely unreasonable numbers.

5.1 Comments

To this point we have been tacitly assuming that antenna patterns with their sidelobes limited effective detection to velocities corresponding to beyond some minimum angle offset from the antenna mainlobe center. This is the classic single-channel GMTI mode, detecting in the exo-clutter region, where the boundary is defined by maximum allowable clutter discrete and the desired RCS detection threshold. As the examples showed, this mode can still be quite viable.

However, to improve upon the performance indicated thus far, we require additional degrees of freedom which we will discuss in subsequent sections.

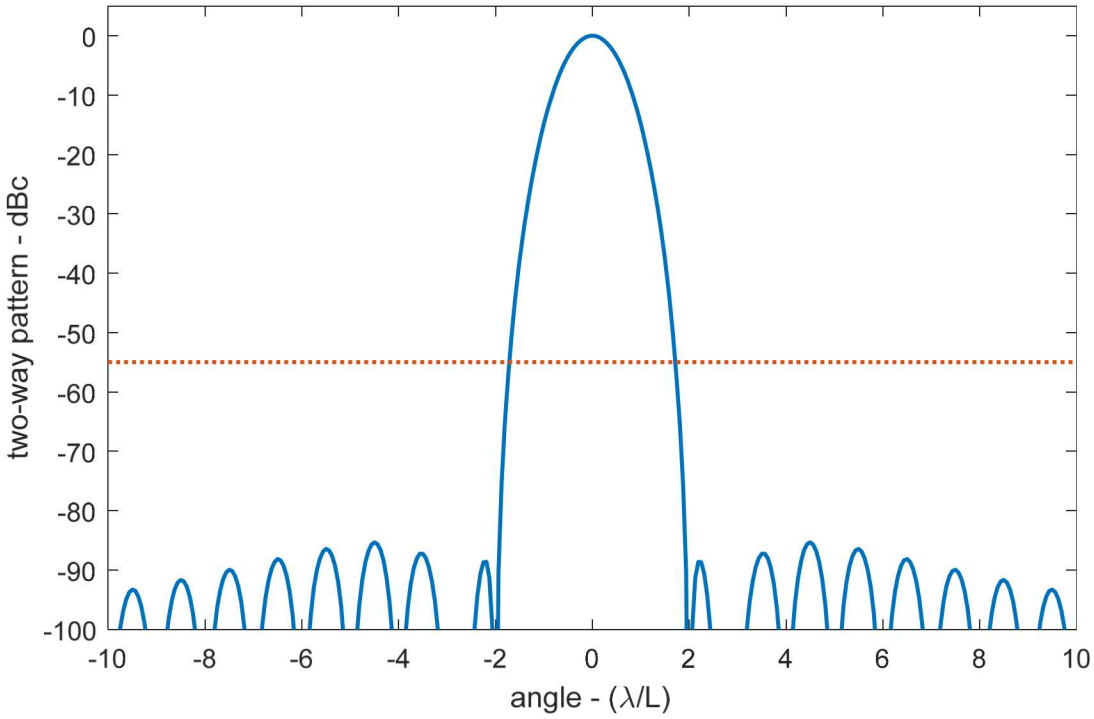

Figure 2. Two-way antenna pattern for Hamming tapered aperture on both transmit and receive.

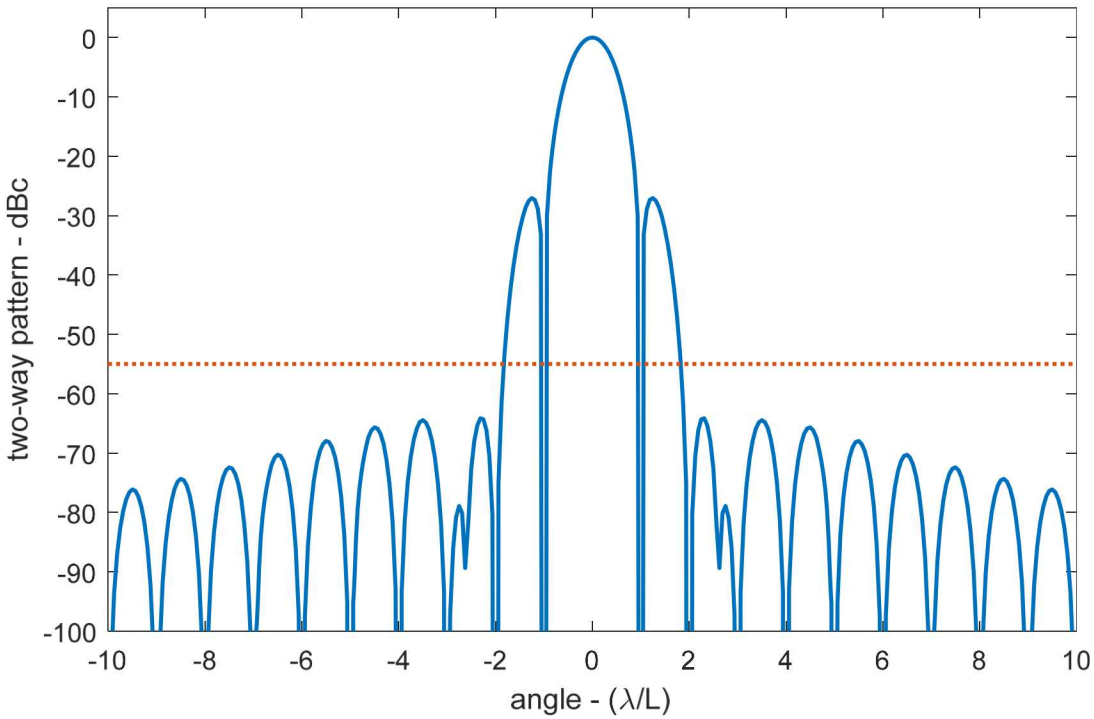

Figure 3. Two-way antenna pattern for Hamming taper on transmit aperture, uniform taper on receive aperture.

6 Angle-Doppler Spectrum

We now engage a more detailed discussion of the relationship between angle and Doppler than was given in Section 4.

We begin with an example range-Doppler map, or image, in Figure 4, where GMTI raw data has been processed to resolve velocity and range. The clutter is clearly not uniform since terrain features are observable in the illuminated portion of the image.

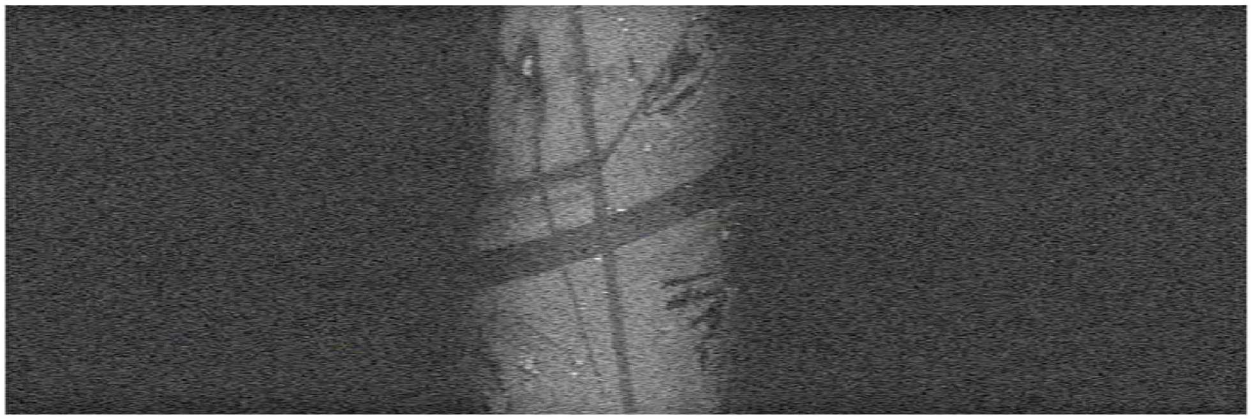

Figure 4. Example of range-Doppler image. Near range is at the bottom edge of the image, and far range is at the top edge of the image. The antenna used was a dish antenna with significant aperture tapering.

More generally, a range-Doppler map of uniform stationary clutter might appear as in Figure 5. An average Doppler profile of such an image might be as illustrated in Figure 6. We note the distinct regions.

> Mainlobe clutter is the clutter manifesting in the mainlobe of the antenna response.
>
> Sidelobe clutter is any obvious clutter not in the mainlobe response; entering the data via the antenna sidelobe response. This is also limited to Doppler regions where the sidelobe energy is above the system noise level. The sidelobe clutter region width will fluctuate as the system noise level changes.
>
> The Exo-clutter region is the Doppler region beyond the obvious sidelobes, where data is dominated by system noise.

The term “endo-clutter” refers to anything that isn’t exo-clutter; includes both mainlobe and sidelobe clutter regions.

Our general desire for GMTI/DMTI radar is for the mainlobe clutter region to be narrow. Furthermore, sidelobe clutter can represent a complication to our processing, so we desire the sidelobe clutter region to be minimally wide.

We note that these definitions are for uniform clutter, and that clutter discretes can appear and be detectable well into the exo-clutter regions, depending on how fast the antenna sidelobes roll off. They can still be a sidelobe problem, even if appearing in the exo-clutter region.

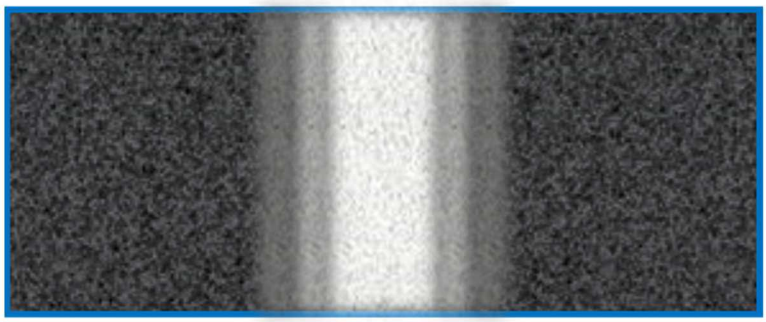

Figure 5. Notional range-Doppler image for uniform stationary clutter.

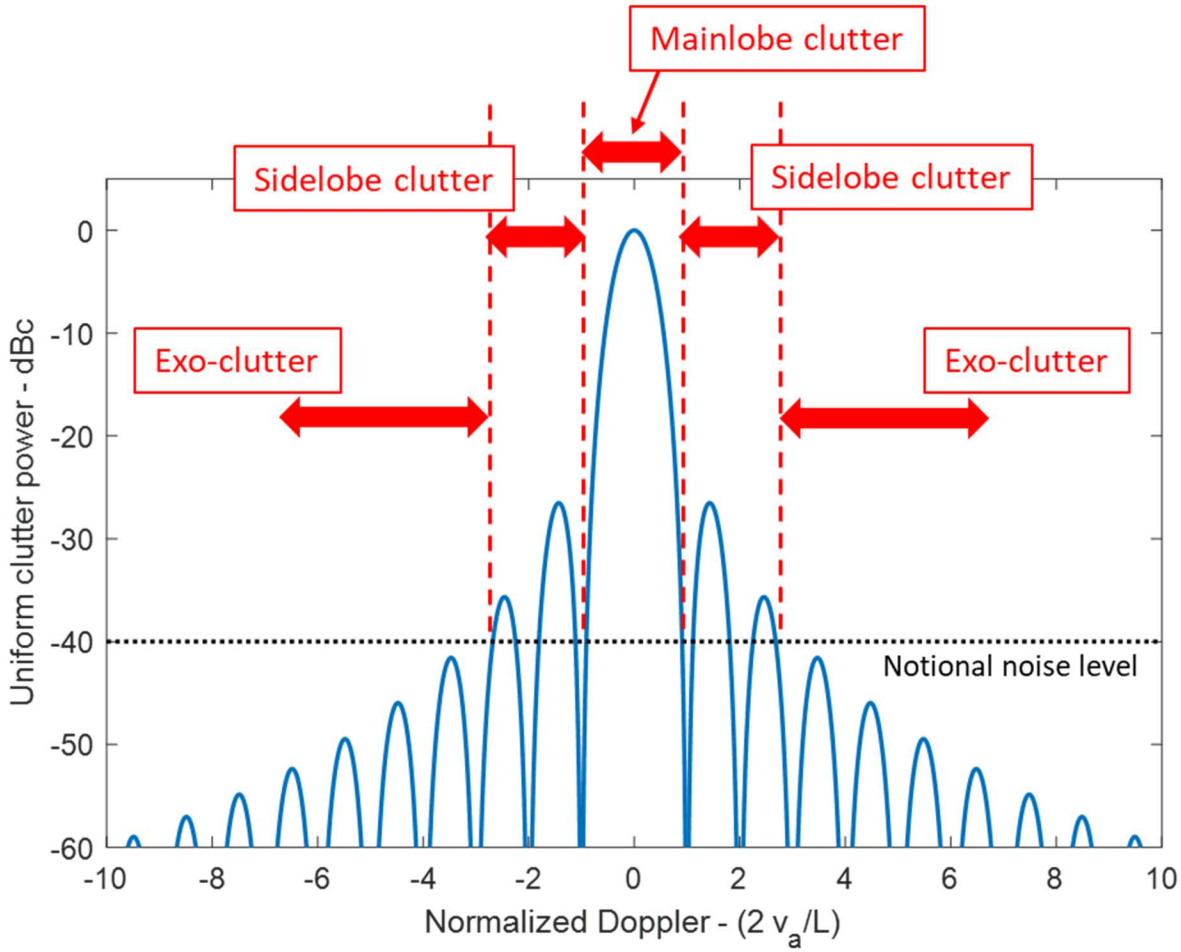

Figure 6. Uniform clutter response regions. Antenna is uniformly illuminated on both transmit and receive, with notional clutter and noise levels. Detection thresholds will be significantly above the noise level.

A more comprehensive discussion of how clutter manifests in a range-Doppler image can be found in reports by Bickel,[13] and by Doerry.[14]

We also make the gratuitous observation that detection thresholds might be made to be Doppler dependent. That is, setting a detection threshold for dismounts at velocities beyond what we can reasonably expect for dismounts, might be somewhat of an excessive expectation for radar performance.

A popular rendering of the relationship between angle and Doppler is the Angle-Doppler Spectrum. From a range-Doppler image exemplified by Figure 4, we begin by selecting a single row of pixels, representing a constant range line, as illustrated in Figure 7.

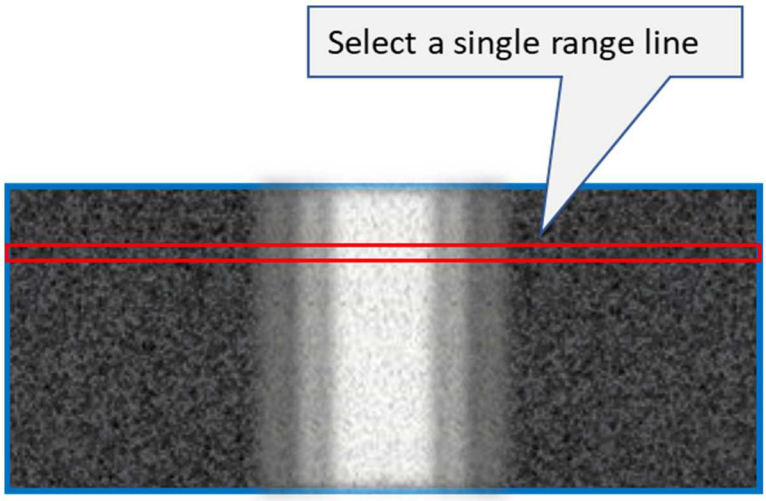

Figure 7. Identified constant range line in notional range-Doppler map of uniform stationary clutter.

6.1 Stationary Clutter

Having selected a specific range line, we continue by rearranging Eq. (12) to the form

$$\sin\theta = \frac{\lambda}{2v_a} f_d \,. \tag{18}$$

Plotting this relationship for uniform stationary clutter of a single range line yields Figure 8. Note that the Doppler spectrum for uniform stationary clutter faithfully reproduces the two-way antenna pattern.

If the clutter in this range line were not uniform, then its brightness variations would have been superimposed onto the Doppler spectrum, as illustrated in Figure 9. This is also true for clutter discretes.

Some observations are key to subsequent analysis.

- For stationary clutter of any sort, for a specific range, there is a single DOA angle for a single Doppler frequency. The mapping is one-to-one. We are ignoring any Doppler processing-sidelobes or other multiplicative noise sources.

- Nulls in the antenna pattern result in nulls in the Doppler spectrum for stationary clutter.

- Stationary clutter has highly correlated and predictable Doppler characteristics. This is true for distributed clutter as well as clutter discretes.

6.2 Moving Targets in Clutter

Consider now uniform stationary clutter with the addition of a single moving specular target, as illustrated in Figure 10. The target is located in a direction that is the same as the center of the antenna mainlobe, but has additional motion to impart additional Doppler to its echo, offsetting its Doppler location from the clutter ridge.

The Doppler spectrum shows the target's response shifted in Doppler. If shifted far enough, to a Doppler spectral region where clutter has been attenuated to the noise level or below, then the target becomes detectable, assuming it is adequately above the noise level itself. A tacit assumption is that Doppler resolution is sufficient to separate or resolve the target energy from the clutter locus.

The real problem is if the target is small, and its velocity shifts its Doppler response but not enough to escape the clutter mainlobe response. This is the DMTI problem. Figure 11 illustrates this case with a zoomed-in antenna mainlobe. Detecting a target embedded within, and comparable with the background clutter becomes intractable with the antenna pattern given. Further complicating this problem would be the presence of clutter discretes.

A key observation is that a different antenna beam pattern will yield different target detection results, especially if the target happens to fall within a Doppler frequency for which the antenna pattern places a null on competing clutter.

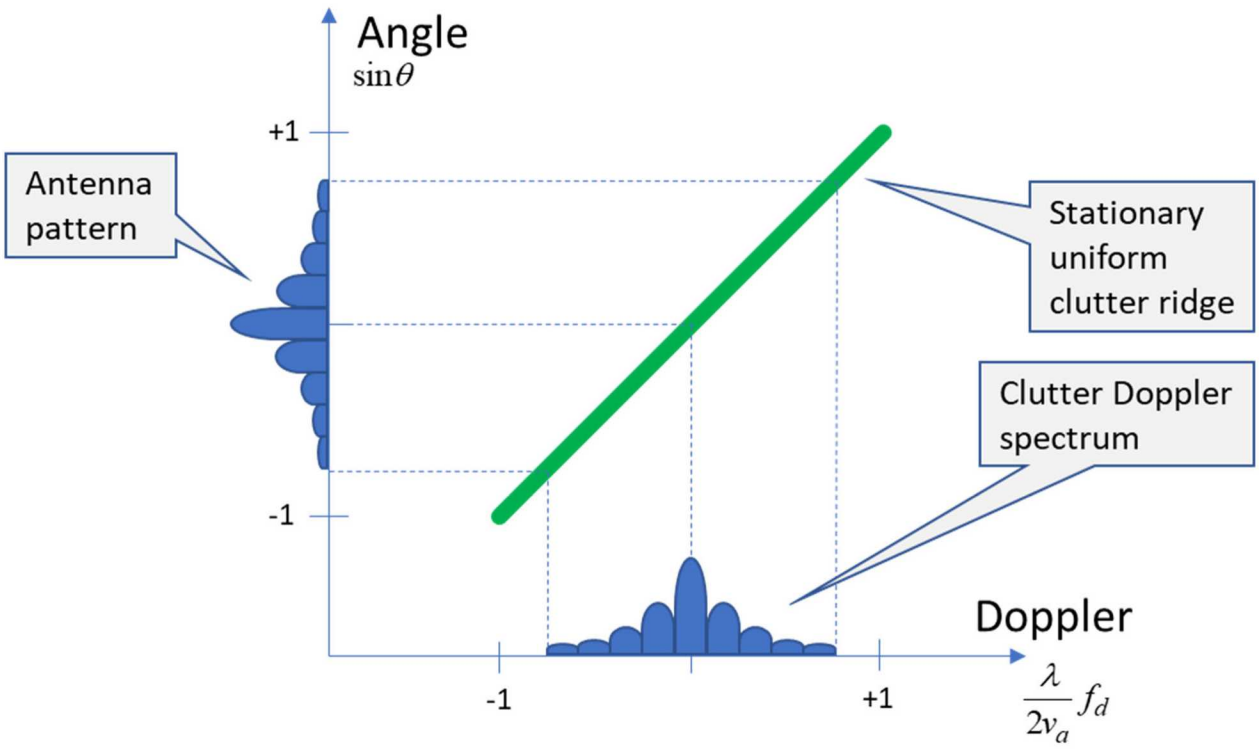

Figure 8. Angle-Doppler spectrum for uniform stationary clutter.

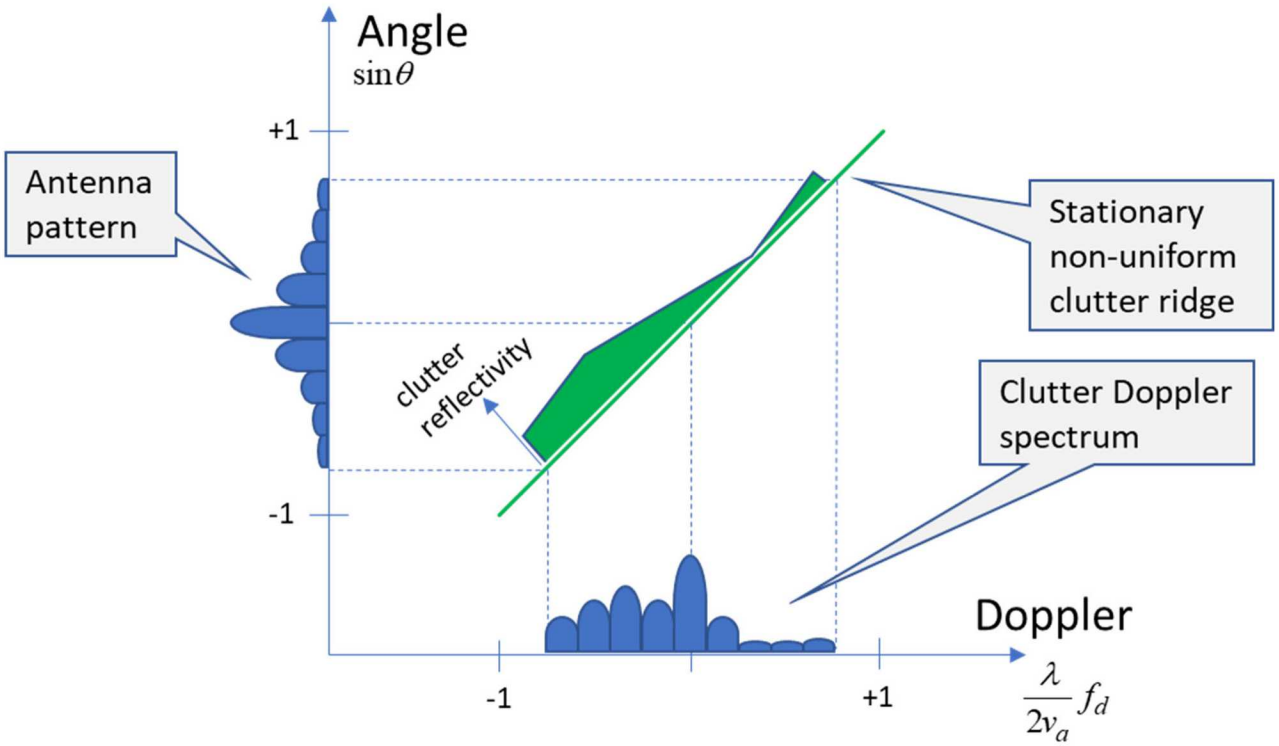

Figure 9. Angle-Doppler spectrum for non-uniform stationary clutter. All stationary clutter is located on the diagonal clutter ridge, but not every location on the clutter ridge exhibits the same clutter reflectivity.

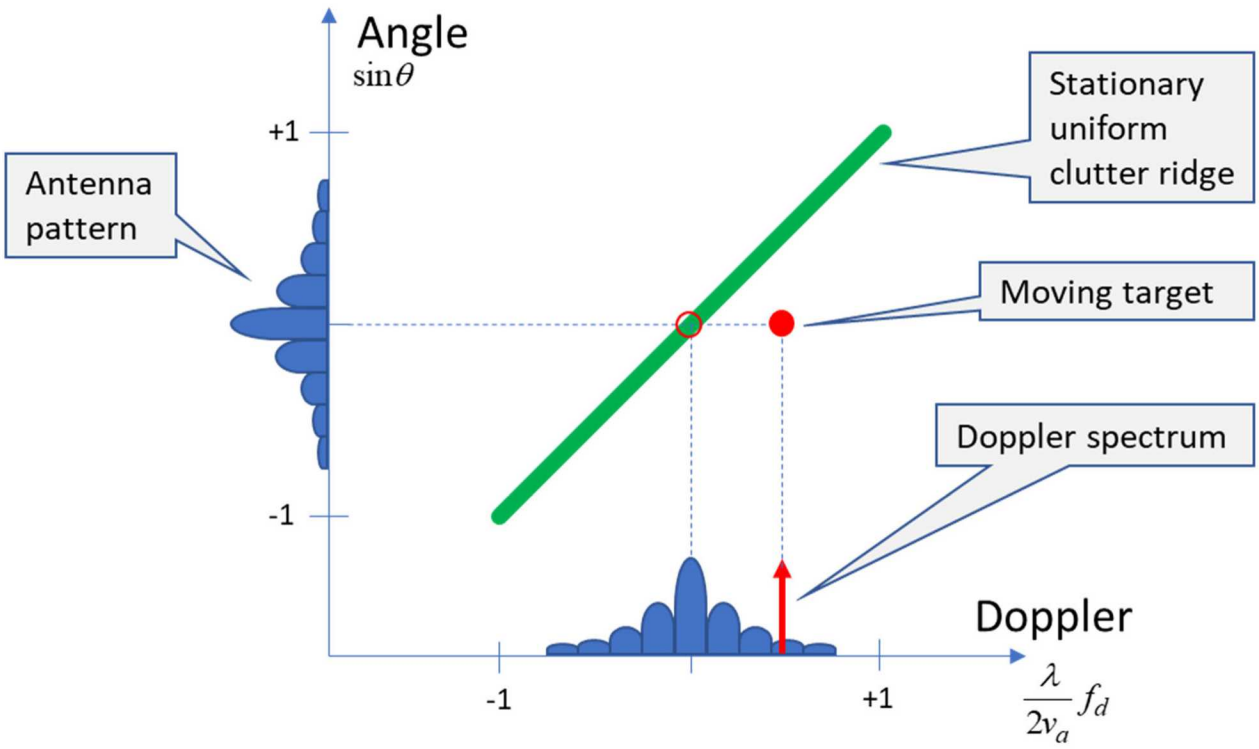

Figure 10. Angle-Doppler spectrum for uniform stationary clutter and single moving target.

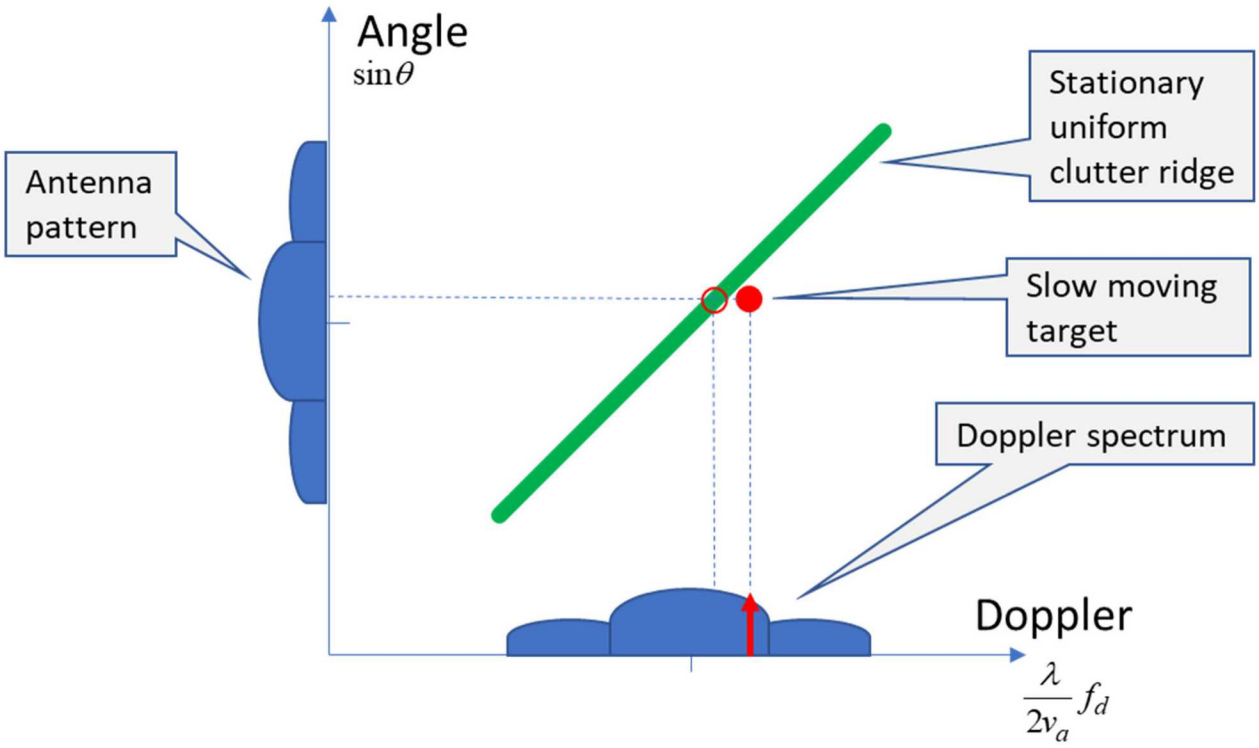

Figure 11. Angle-Doppler spectrum for uniform stationary clutter and single small slow-moving target.

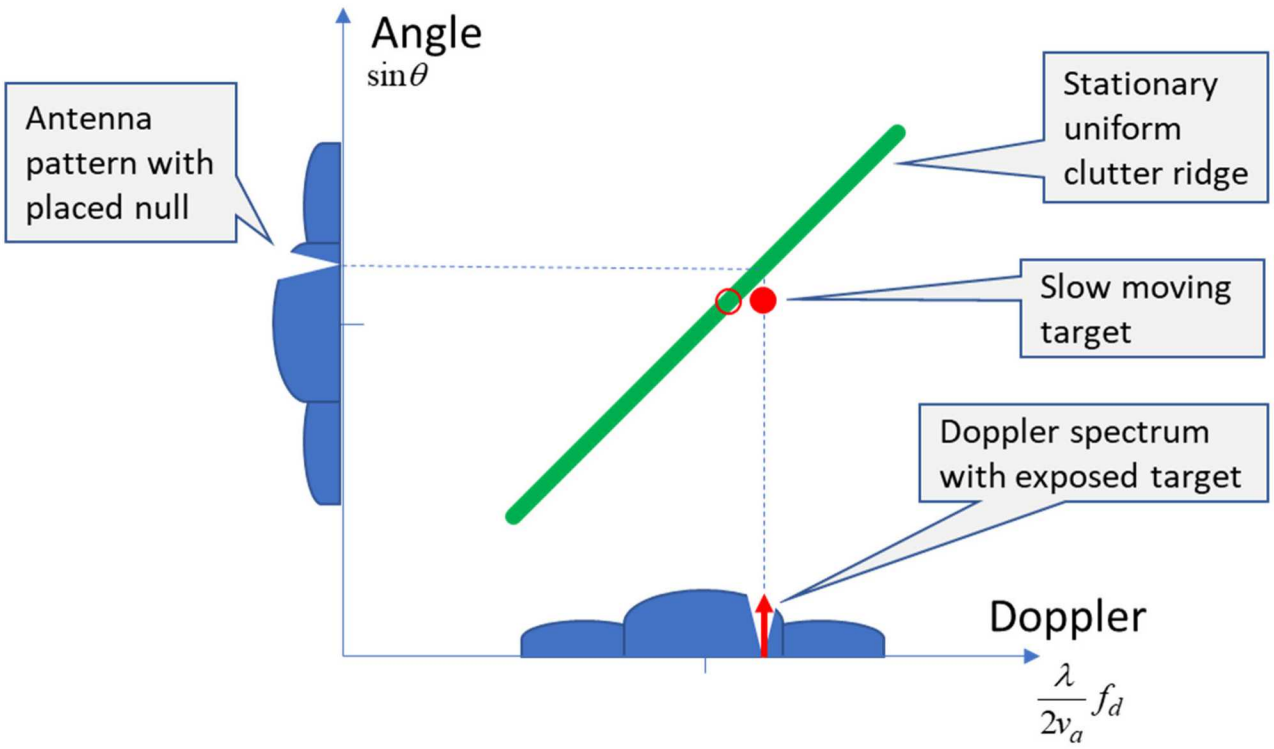

Figure 12. Angle-Doppler spectrum for uniform stationary clutter and single small slow-moving target, with modified antenna pattern. This illustrates how a spatial antenna pattern null can manifest as a Doppler frequency null for stationary clutter. A moving target exhibiting the same Doppler as stationary clutter in the null will have a different DOA, and hence not be affected, at least as much, by the antenna pattern null.

6.3 Beamforming (Null Steering)

As previously noted, nulls in the antenna pattern result in nulls in the Doppler spectrum for stationary targets. Moving targets, although perhaps exhibiting the same Doppler, actually reside in a direction that is different for that particular null, and hence become observable. This is illustrated in Figure 12.

To summarize, if we find energy at a Doppler frequency where we should have none from stationary clutter, then that energy must be due to a moving target. Consequently, it becomes desirable to create and place a null in the two-way antenna pattern at will. This programmability of the antenna pattern requires programmability in the aperture illumination function, which in turn requires an additional degree of freedom from a fixed single phase-center or single-beam antenna.

In practice, the beam modification to place a null is done with the receive antenna rather than the transmit antenna. Since the two-way pattern is a product of the two, a null in the receive antenna will also be a null in the two-way pattern. The receive antenna is chosen because, for example, if separate samples of the aperture (i.e. subapertures) can be individually digitized and stored, then the composite beam can be formed using data processing, and the stored data can be reused to form many different beams to move the notch appropriately as needed after the fact.

There are limits to the notch width due to the physical size of the antenna, and the proximity of the moving target Doppler to the notch will affect the target's detectability, which ultimately is embodied into a Minimum Detectable Velocity (MDV), as presented in a paper by Bickel and Doerry.[15]

The concept of steering nulls to discriminate moving targets from stationary clutter is central to most high-performance DMTI/GMTI radar detection algorithms. Collectively, they are termed "Space-Time Processing." We examine some basic classes of algorithms very briefly next.

6.4 Space-Time Adaptive Processing (STAP)

As the name suggests, STAP is an "adaptive" process to the data at hand. The intent is still to modify the receive antenna beam to mitigate clutter so that a competing moving target can be exposed and detected, as in Figure 12.

The antenna beam pattern is modified by weighting subapertures to suppress stationary clutter (and any other interferers) at some DOA. Clutter is not nulled, per se, but rather attenuated to the noise level, as part of an optimization process usually to maximize SINR for a moving target in a particular direction. This is often referred to as a whitening process. Where in angle space and how much to attenuate clutter is estimated by examining a presumed target-free region in the neighborhood of the range-Doppler cell under test. This data-driven estimation and resulting filtering is the "adaptive" part of STAP.

Much has been written about STAP, with a book by Guerci being a good reference.[16] Many variations of STAP algorithms exist. A more detailed discussion of STAP, and all its forms, is beyond the scope of this report.

6.5 Displaced Phase Center Antenna (DPCA) Processing

The fundamental concept for DPCA processing is to collect two CPIs of data displaced slightly in time, but otherwise spatially coincident. Stationary clutter is coherent, in fact identical. Only a moving target and noise will be different between the two range-Doppler images. Since there is no effective motion between the two CPIs, the net radar velocity is effectively zero. Consequently, subtracting one image from the other should "cancel" all clutter en masse, over the entire antenna beam footprint with sidelobes and all, at least to the noise level, but leave residual energy from the moving targets. A good introduction to DPCA processing is given in a text by Schleher.[17] We emphasize that the intent is to cancel 'stationary' clutter. Any clutter motion can still be somewhat problematic.

The two separate CPIs necessitate two distinct antenna phase centers or equivalent. It is also generally assumed that the independent CPIs are formed with identical antenna gain patterns, which may be problematic, perhaps requiring additional processing.

With respect to the Angle-Doppler spectrum, subtracting one image from the other is like forcing a notch along the entire clutter ridge itself. Moving targets have a non-zero Doppler due to their

own motion, and are not on the clutter ridge. They offer differences between the two CPIs, and hence are not completely cancelled, and hence detectable. This is illustrated in Figure 13.

There may also be complications when the antenna baseline (the line segment connecting the phase centers) is not oriented parallel to the radar flight direction, but these can be overcome (compensated) with additional processing. This algorithm has much in common with Coherent Change Detection (CCD) processing of Synthetic Aperture Radar (SAR) images.[18]

More generally, DPCA is about implementing a spatial alignment of phase centers, by/with attendant temporal offsets, to filter/discriminate moving targets from stationary clutter. DPCA algorithms require at least two phase centers, but may employ more than two phase centers.

6.6 Along-Track Interferometry (ATI) Processing

As the term "interferometry" implies, ATI is about measuring DOA angles with respect to the nominal antenna broadside direction. For a particular range-Doppler cell, the expected DOA for stationary clutter is calculated, perhaps an average DOA of surrounding clutter pixels. Independently, the DOA for that cell is measured, with all DOA measures being interferometric measurements using multiple beams or phase centers. The interferometric measure is a phase measurement. These DOA's are effectively compared, and any significant dissimilarity indicates a moving target. This is illustrated in Figure 14.

We stipulate that the range-Doppler cell for which a DOA measurement is made, if containing both target and clutter, will exhibit a phase corresponding to a DOA somewhere in between the clutter direction and target direction. Just exactly where in between the measured DOA will indicate depends on the relative strengths of the respective echoes.

The presumption is that the DOA offset is measurable as a monotonic, nearly linear phase shift. This characteristic is reasonably good within the mainlobe of the antenna beam, especially the center section of the mainlobe, but falls apart in the sidelobe region where phase shifts tend to jump across antenna nulls and are not guaranteed to be otherwise well-behaved.

6.7 Comments

We make some ancillary observations here.

- It is well-known and easily shown that accurately locating target DOA in clutter requires the ability to steer two or more nulls; an architecture with three or more phase centers, or beams.[19]

- While antennas can be constructed with separate beam directions from a common phase center,[20] the more common architecture is subapertures with distinct phase centers.

- When employing an antenna with distinct phase centers, it is imperative to precisely ascertain just where those phase centers are. Especially when tapering is employed, the phase centers may not be in the center of the subapertures.[21,22]

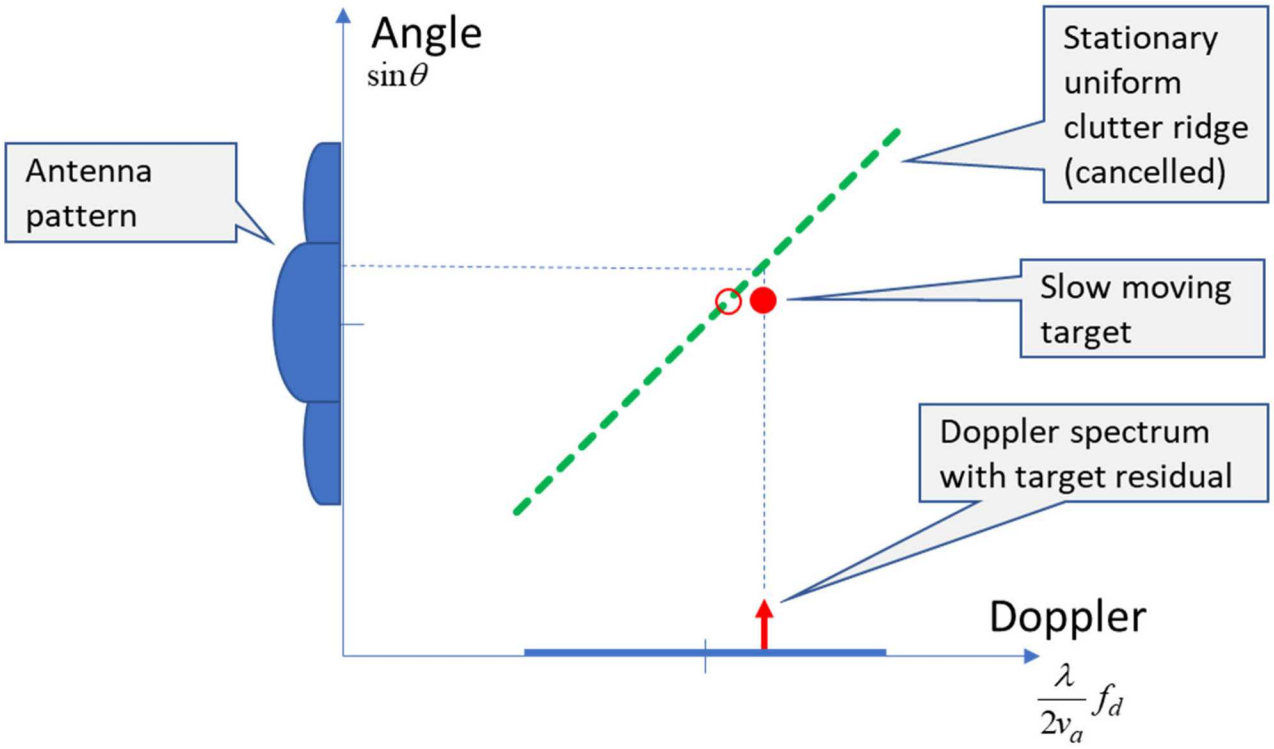

Figure 13. Angle-Doppler spectrum for uniform stationary clutter and single small slow-moving target, assuming DPCA processing.

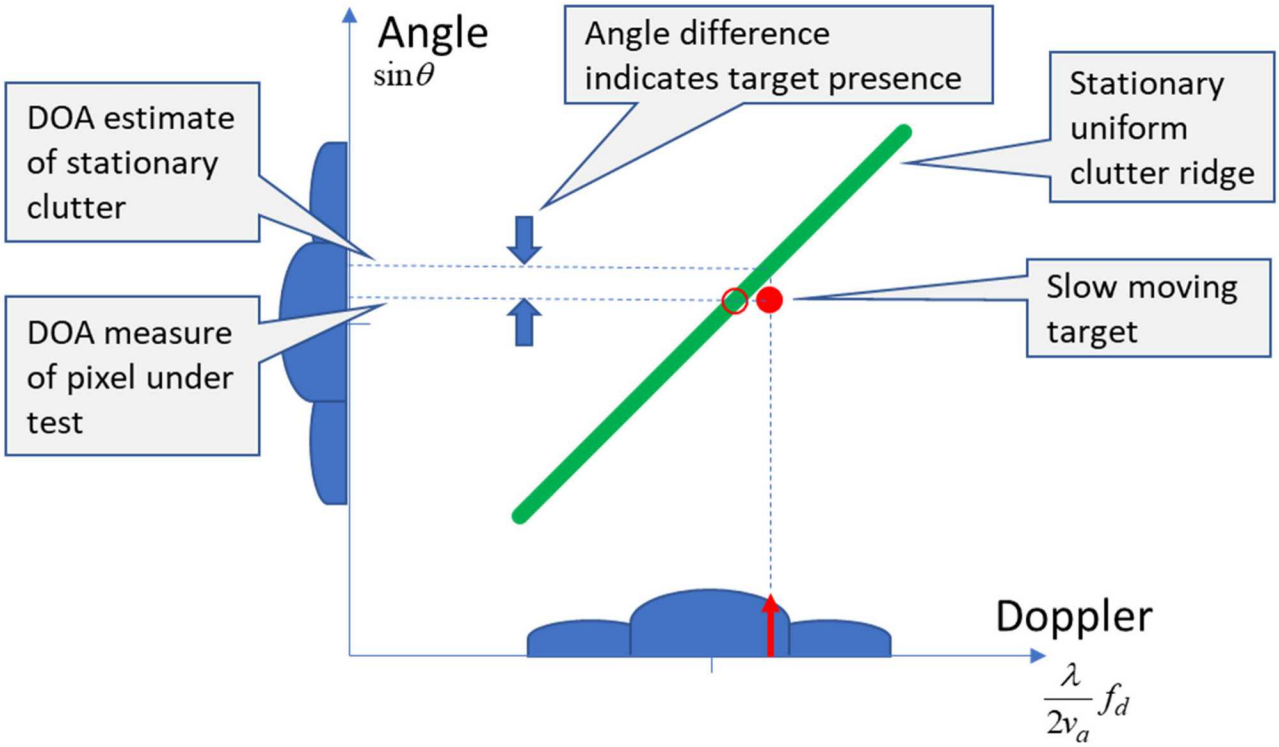

Figure 14. Angle-Doppler spectrum for uniform stationary clutter and single small slow-moving target, showing ATI measurement.

7 Antenna Sidelobes Revisited

Referring again to Figure 6, we now revisit the issues that antenna sidelobes present to us.

Preferably, the antenna's sidelobe response would be such that all stationary clutter in the sidelobes (both distributed and discrete) would be rendered to below detection levels, and ideally to below the noise level. Any clutter that is above our detection threshold becomes problematic for us.

Our options for dealing with clutter that "leaks" through the antenna sidelobes becomes

1. Suppressing sidelobe energy before any detection process, and/or

2. Suppressing/ignoring erroneous detections due to sidelobe energy (after detection).

Of course, the more we can suppress before detection, the less we have to deal with after detection.

Our ability to engage either of these mitigation techniques will depend on the specific DMTI/GMTI processing employed, and the availability of potentially additional antenna features.

We note without elaboration that while we discuss in this report mitigating clutter, many of the following techniques work well for interference, intentional and otherwise.

7.1 Pre-Detection Techniques

In the sidelobe clutter region, both distributed and discrete clutter can manifest with enough energy to be detectable. However, because the specific nature of observed clutter is unpredictable, neither is guaranteed to manifest at all.

In the exo-clutter region, we can reasonably assume that distributed clutter will not manifest to detectable levels. However, clutter discretes might still be strong enough to exceed our detection thresholds. They will then appear in the range-Doppler map as false moving targets, which is undesirable.

7.1.1 Conventional Processing

Pre-detection techniques for dealing with clutter entering the antenna sidelobes are generally those outlined in Section 6. We comment on them here.

Null-steering should work well even for stationary clutter manifesting in the antenna sidelobes. That is, nothing prohibits us from placing a null in a direction illuminated by an antenna sidelobe. However, a mechanism for determining clutter DOA still needs to be determined, that is, the DOA at which stationary clutter actually appears. This might be calculated from radar geometry, assuming factors like antenna pointing and scene topography can be determined with adequate accuracy and precision.

An adaptive algorithm like STAP typically needs good Clutter to Noise Ratio (CNR) for a suitable neighborhood around range-Doppler cell to properly calculate an adequate clutter filter. STAP works best for homogeneous clutter, often exhibiting difficulty with nonhomogeneous clutter including clutter discretes. STAP may have difficulties with the sidelobe clutter region if adequate CNR is not achieved. STAP, typically needing good CNR for a neighborhood around range-Doppler cell, is likely not suitable for clutter discretes in the exo-clutter region.

DPCA attempts to place a true null onto all clutter en masse, regardless of clutter strength. In principle, it does not require adaptation in the way that STAP requires, so does not rely on neighboring clutter characteristics. Consequently, DPCA should cancel clutter even in sidelobes, limited only by system errors, imbalances, and noise. As a practical matter, the word 'cancel' really manifests more like a substantial attenuation.

ATI must contend with phase wraps and ambiguities commonly associated with any phase-difference measurements in addition to SNR limitations. This can present difficulties with discriminating sidelobe clutter.

7.1.2 Sidelobe Cancellation (SLC)

A technique used to specifically steer a null towards sidelobe energy is termed "sidelobe cancellation." This technique normally employs a wide-beam secondary antenna intended to capture sidelobe energy, which is then scaled and subtracted from the principal antenna's response, thereby 'cancelling' sidelobe energy in the principal antenna's received signal.

The secondary wide-beam antenna is often called a "guard" antenna, and its signal is processed by a "guard channel."

Proper gain and phasing of the subtracted signal is often adaptive, and such a system is called an "adaptive sidelobe canceller." Multiple guard channels might be employed to place multiple nulls, each in a different direction.

Farina, in Skolnik's Radar Handbook,[23] offers a good introduction into adaptive SLC operation. Mao also addresses the topic in some detail in a text edited by Galati.[24]

7.2 Post-Detection Techniques

Post-detection techniques, as the name implies, are processing algorithms applied to preliminary target detections. These techniques implement additional testing to discriminate a true moving target detection from clutter entering a sidelobe. They are sometimes referred to as False Alarm Mitigation (FAM) techniques.

7.2.1 Sidelobe Blanking (SLB)

As with SLC architectures, sidelobe blanking employs a guard antenna and a guard channel. The essential premise for sidelobe blanking is that energy in the sidelobe region for the principal antenna is compared to the manifestation of the same energy source in the lower-gain mainlobe region of the guard antenna response. If the guard channel signal is greater than the principal

antenna's response, then the energy is indeed a sidelobe response, and it is ignored, or "trimmed" from the list of legitimate detections. A typical guard channel response is exemplified in the pair of plots in Figure 15. The relative gain of the guard channel to the principal antenna can be adjusted with amplification or attenuation.

In other arenas, such trimming of sidelobes is termed "apodization." Consequently, SLB algorithms have much in common with sidelobe apodization algorithms.[25]

A legitimate question emerges that "If algorithms exist to ostensibly filter sidelobes in their entirety, then why would we ever need a guard channel?" A reasonable answer is that since not all algorithms will adequately cancel or otherwise mitigate clutter energy, limited perhaps by non-ideal hardware, it is prudent to retain options. As such, a guard channel is a reasonable option for target/clutter discrimination.

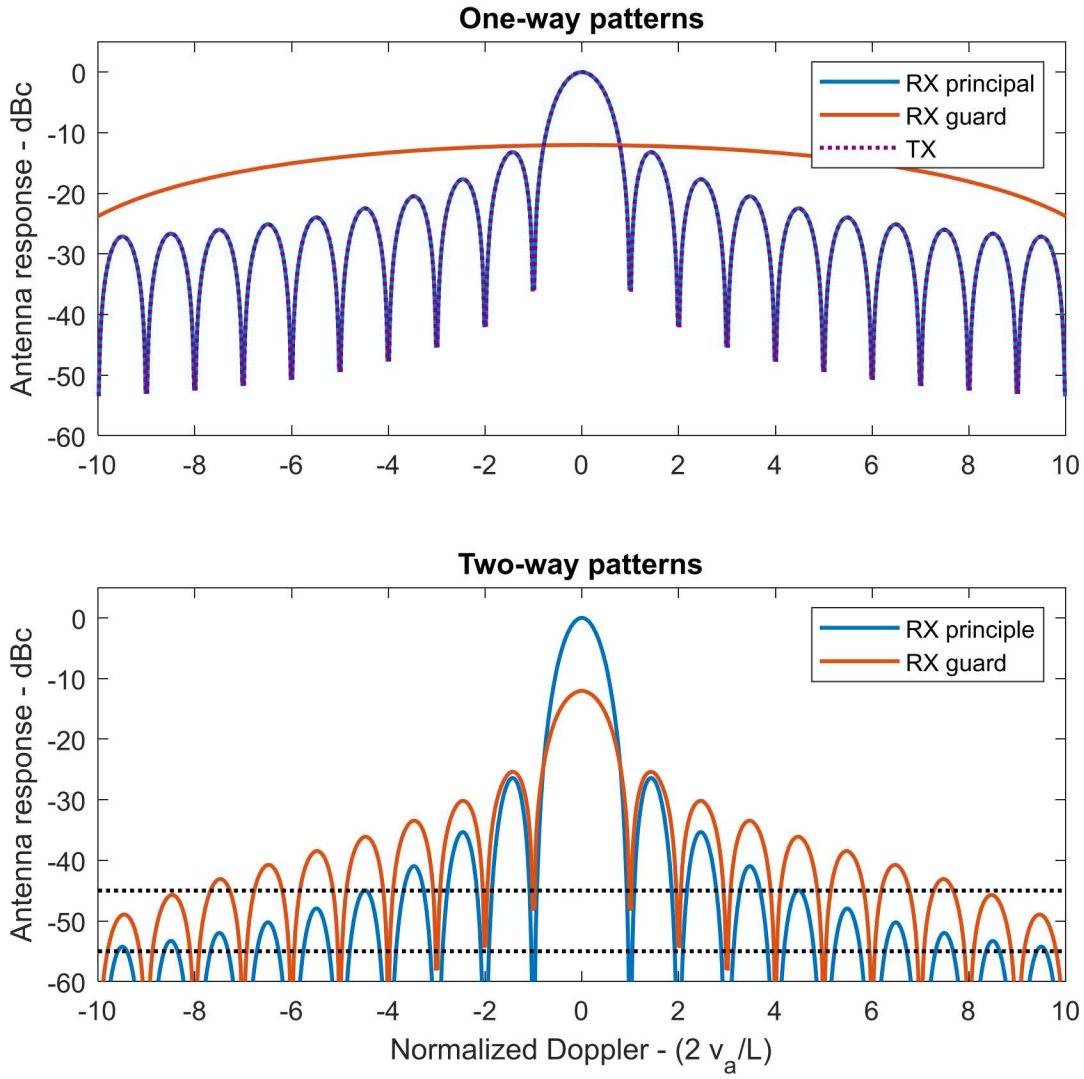

Figure 15. Classic guard channel antenna patterns. Only in the region of the principal antenna mainlobe does the principal antenna response dominate the guard antenna response.

The essential characteristic of a guard channel is that it provides a greater response to received energy in directions where the principal antenna's sidelobes are problematic. The guard antenna's pattern needs not necessarily to offer a particular shape, say a sinc function. For example, a monopulse difference channel may suffice in some applications, as is notionally illustrated in the pair of plots in Figure 16. Its relative gain to the principal antenna can also be adjusted with amplification or attenuation.

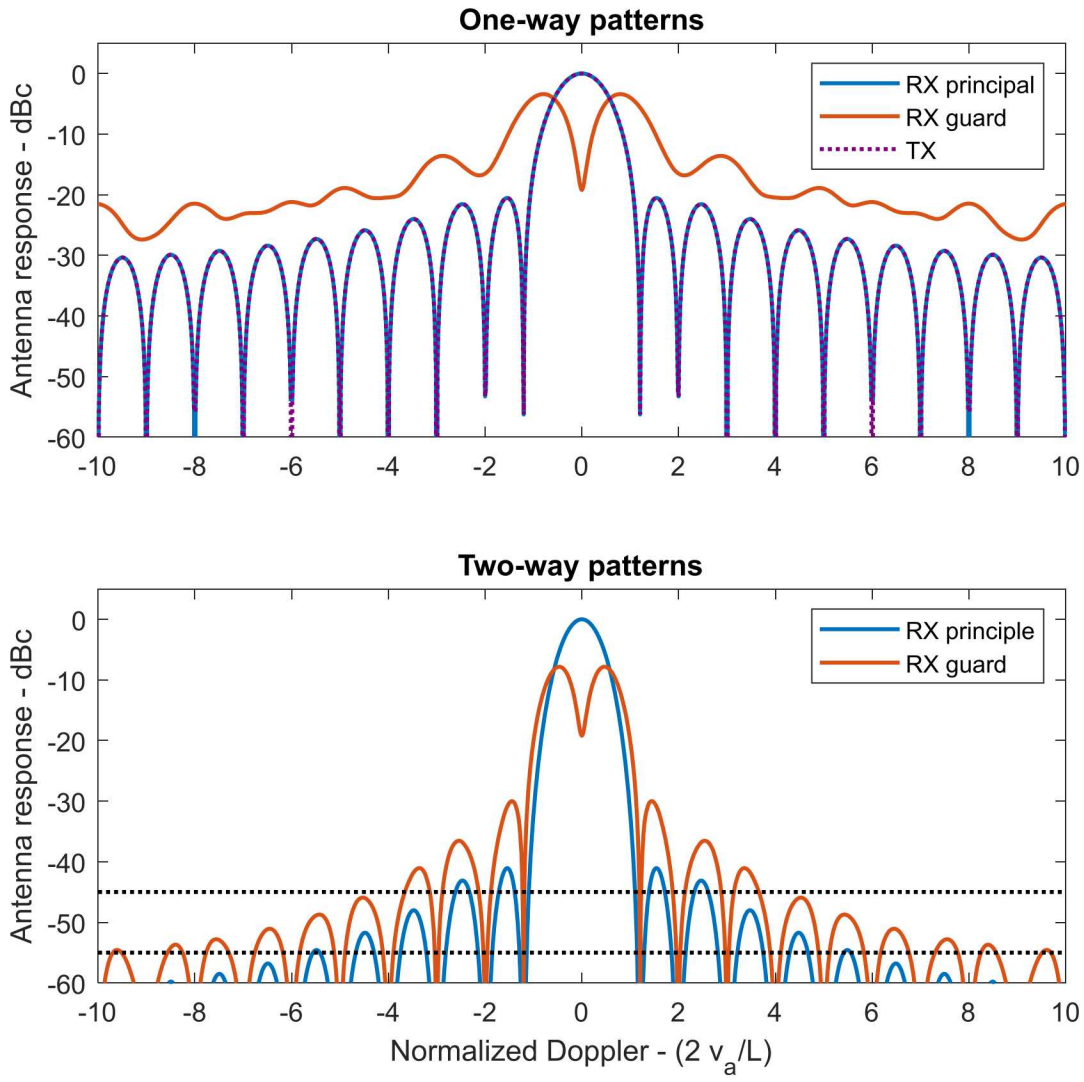

Figure 16. The monopulse difference beam may sometimes be used as a guard antenna. Note that the guard channel's response remains above all relevant sidelobes of the principal antenna.

7.2.2 Scan-to-Scan Processing

The behavior of target detections over multiple CPIs, including multiple scans, might be used to discriminate legitimate moving targets from clutter. For example, targets that translate (i.e. move in position) are probably not stationary clutter, discrete or otherwise.

A subset of scan-to-scan processing is target tracking, which we call out separately next.

7.2.3 Target Tracking

The value of GMTI/DMTI radar is substantially enhanced when coupled with target tracking, which essentially ties together a time history of target detections to discern time-dependent behavior. Obviously, the track of a vehicle or dismount exhibits significant differences from that of a clutter discrete.

Target tracking is a rich area, well represented in the literature. A good place to begin a more thorough investigation is with a presentation by Crouse.[26]

7.2.4 Micro-Doppler Signatures

While it is convenient to model moving targets as rigid bodies, with all components exhibiting constant identical motion, in fact many targets are decidedly not so. Such non-rigid motion leads to micro-Doppler signatures, essentially measures of non-uniform velocity and accompanying Doppler variations, that similarly varies with time. Micro-Doppler signatures might be used to discriminate between target classes, and target from clutter.[27,28]

For example, vehicles might display moving tracks, or rotating wheel hubs, as shown in Figure 17.

A walking dismount exhibits articulated limbs with respect to the torso, typically periodic with gait. The Doppler signature of a walking dismount is quite distinct from a typical clutter discrete.[29] A typical spectrograph is shown in Figure 18.

A composite heat-map of range-Doppler images of a walking dismount typically shows a distinctive “waddle” with time, as illustrated in Figure 19.

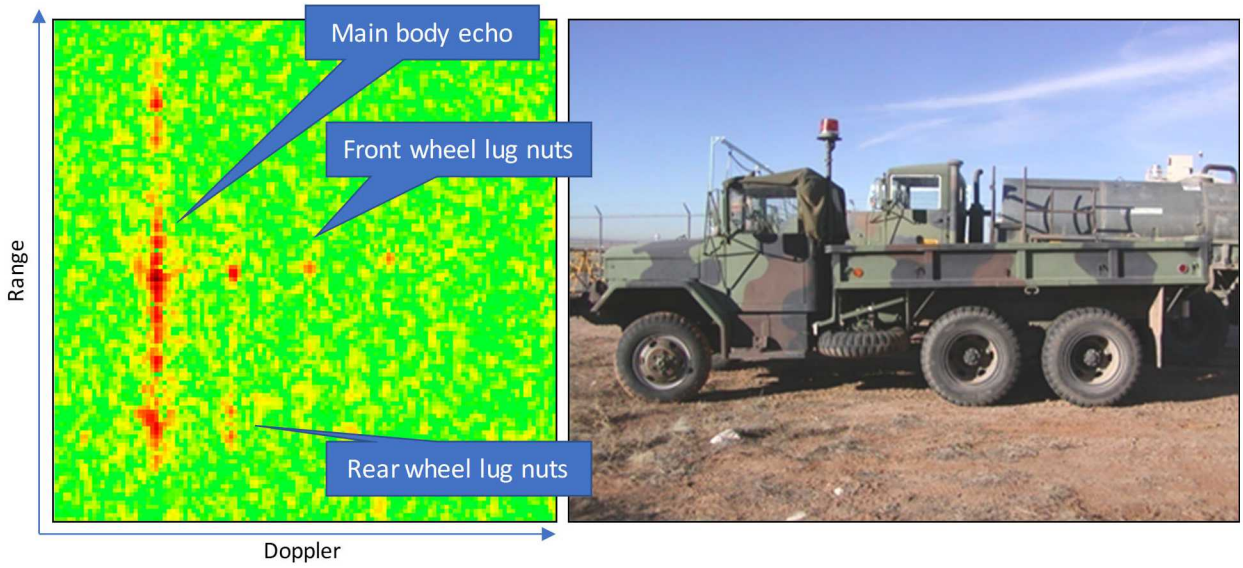

Figure 17. Range-Doppler response of 2.5 Ton truck exhibiting micro-Doppler signatures. Data collected with Sandia National Laboratories testbed radar.

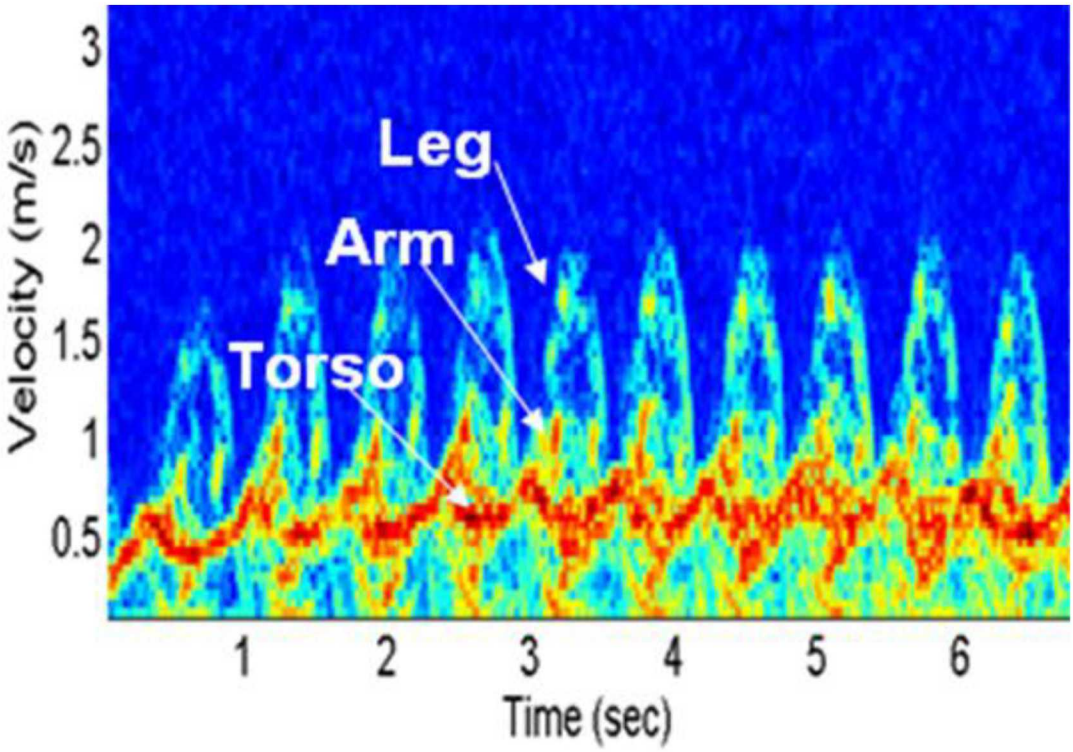

Figure 18. Spectrogram of walking person taken by a radar at Ku band. (source: Tahmoush[29])

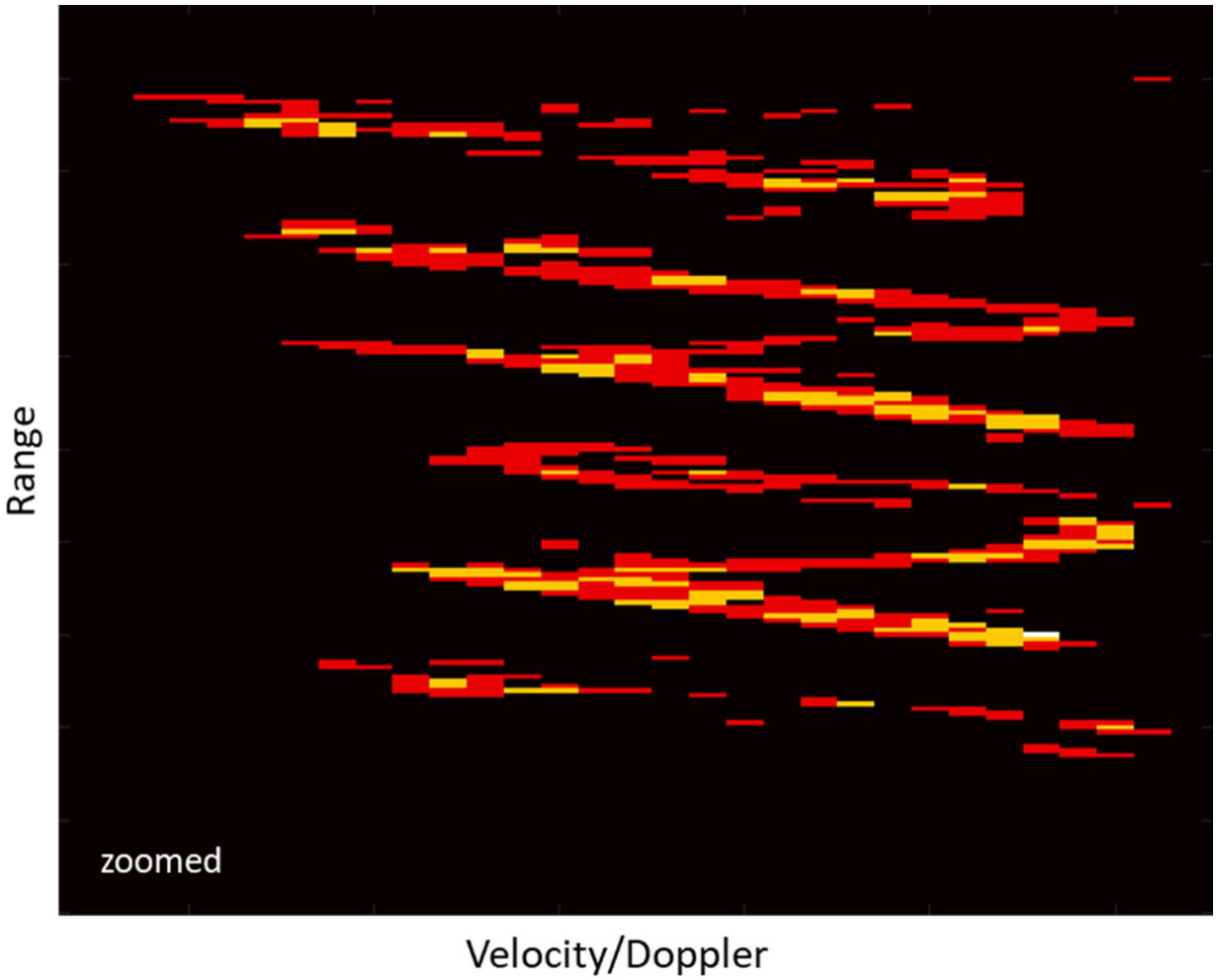

Figure 19. Composite heat-map of range-Doppler image chips showing "waddle" of dismount signature. The Doppler oscillates with time as the dismount's walking causes the range to change with time.

7.2.5 Other

Without elaboration, we simply state that other radar echo features might be useful to separate targets of interest from clutter.

Exploiting road network databases might also be used to ignore detections in otherwise uninteresting locations.

When fine range resolution is employed, target features and characteristics might become observable, and useful for discrimination from clutter. This is sometimes referred to as High Range Resolution (HRR) operation. Figure 17 is an HRR range-Doppler image.

In some circumstances the radar shadow of a detected target might be exploited.

If a target can be discriminated to be flying, perhaps with an elevation DOA measurement, then it may too be characterized as a "mover."

7.3 Comments

The measurements necessary for detecting moving targets depend on comparing echo signals, presuming any processing channels are ideal, in the sense of not interfering with the necessary measurements.

We make some ancillary observations here.

- Ultimately, any antenna beam characteristics, especially those involving precise null steering and DOA estimation, must contend with the entire Electromagnetic (EM) radiation environment, including antenna mounting, occlusion effects, and radome characteristics.

- Channel balancing is an imperative. Any differences in channel characteristics need to be measured and compensated.[30] This is essentially a calibration operation.

- The various algorithms have different capabilities with respect to sidelobe clutter. The need for mechanisms to deal with clutter after detection will depend on the degree with which sidelobe clutter can be mitigated before detection.

8 Design Examples

We now tie the principles discussed in the previous sections together into examples of some candidate designs. We shall presume that our fixed constraints are as follows.

- We wish to design a GMTI/DMTI radar to operate in the Ku-band with 18 mm wavelength.
- The radar is expected to fly at up to 100 m/s.
- The antenna is to be limited in width to 1.0 m.
- The system needs to detect dismounts to −10 dBsm, travelling at 0.5 m/s.
- The system needs to mitigate false alarms due to clutter discretes as strong as +45 dBsm.

Broadside to the flightpath, even a uniformly illuminated antenna beam will nominally illuminate ground clutter with up to 1.8 m/s between its first nulls. This means we need to employ endo-clutter processing.

Accordingly, we will choose

- The antenna will manifest 3 phase centers to facilitate DOA measures in the presence of clutter.
- We will require at least 55 dB sidelobe clutter attenuation or suppression.

8.1 Design Example #1 – Taper on TX Only

Our first example will use a Hamming aperture taper on transmit, and uniform taper on receive, with attendant 1.35 dB relative SNR loss. The RX antenna will be divided into 3 identical subapertures.

The two-way beam pattern exhibits sidelobes as strong as –31 dBc. Consequently, we require a guard channel. With an additional amplification of 3 dB, the center subaperture could suffice as a guard antenna. This is displayed in Figure 20. While this example uses a Hamming taper on transmit, we caution that the nature of the sidelobe suppression is highly dependent on the exact taper employed. Whatever taper is actually achieved in an antenna design will need to be evaluated for its goodness, and whether additional or alternate sidelobe mitigation schemes might need to be employed.

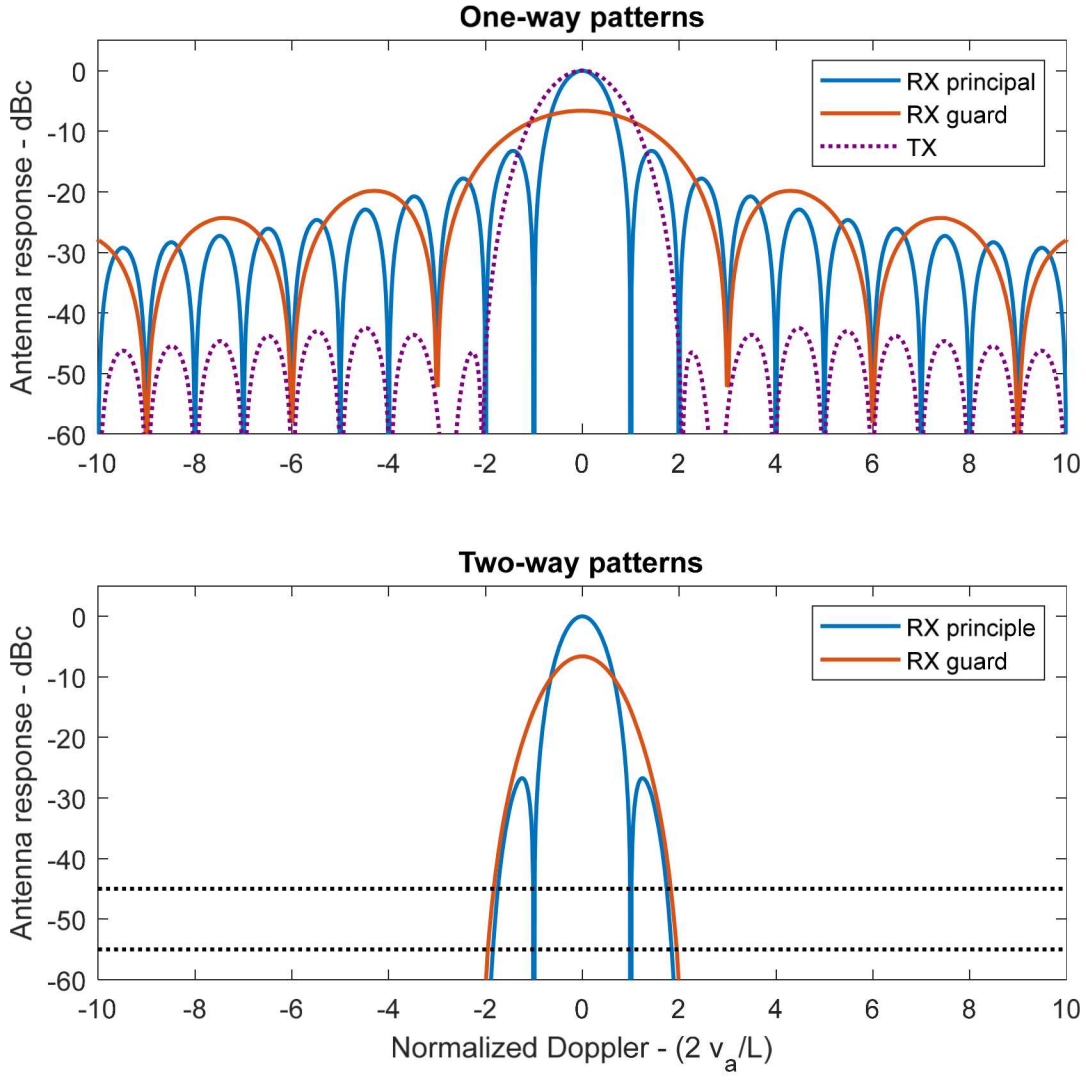

Figure 20. Example antenna patterns with Hamming taper on transmit, and uniform taper on receive.

8.2 Design Example #2 – Uniform Taper on TX and RX

Our second example will use a uniform aperture taper on both transmit and on receive, yielding maximum gain. The RX antenna will be divided into 3 identical subapertures.

The two-way beam pattern exhibits sidelobes as strong as –26 dBc. Consequently, we require a guard channel. We will architect the center subaperture to be an azimuth phase-monopulse antenna, and use the difference channel as the guard channel for sidelobe clutter, with a relative amplification of 9.5 dB. This is displayed in Figure 21.

Note that this configuration requires a fourth signal channel to accommodate the center subaperture difference channel.

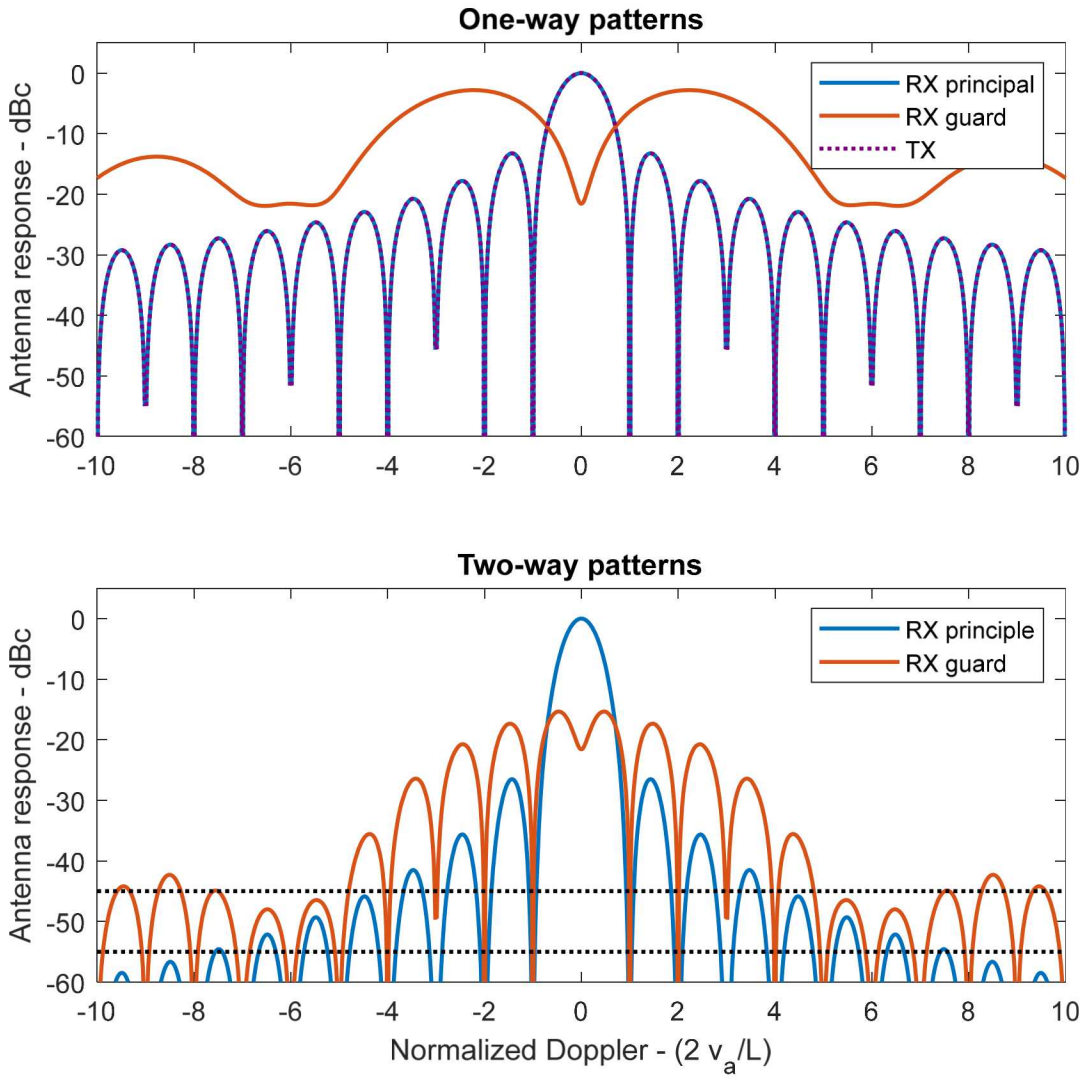

Figure 21. Example antenna patterns with uniform tapers on both transmit and on receive.

"Who are you going to believe, me or your own eyes?"
-- Groucho Marx

9 Comments on 2-D Aperture in a 3-D World

In previous sections we made the presumption of a linear aperture "aligned with the radar's direction of travel." This is essentially a 1-D antenna with subsequent analysis in a 2-D plane. We now make some comments about a 2-D antenna in a 3-D space.

- A finite aperture dimension in elevation will generate elevation sidelobes. In general, clutter in elevation sidelobes can be time-gated out, especially in low-PRF systems. For medium and high-PRF systems, especially with range ambiguities nearer the range of interest, such sidelobes may become significant. A particularly strong echo, compounded by nearer range, is the nadir response.

- Precision elevation DOA measurements require displaced phase centers in the elevation direction. Such measurements are particularly useful for height measurements (e.g. ground-clutter topography), or discriminating flying objects from those on the ground.

- A somewhat optimum arrangement of azimuthal phase centers is oriented parallel to the horizontal velocity vector of the radar. When this occurs, direct DOA measures from the phase centers coincide with DOA measured from Doppler of stationary clutter. When this does not occur, then these two DOA measures may not coincide, especially in squinted (non-broadside) directions, and for non-flat clutter scenes. Processing may become more difficult, but not impossible.

- Knowledge of scene clutter topography can help mitigate DOA ambiguities. Topography might be derived from on-board maps and/or databases, or from independent elevation DOA measurements.

“I realize that I'm generalizing here, but as is often the case when I generalize, I don't care.”
-- Dave Barry

10 Conclusions

We repeat some key points.

- A bane of GMTI/DMTI systems is ground clutter, both distributed and discrete.
- When clutter manifests in antenna sidelobes at sufficient levels to be detectable, it may be illegitimately detected as a target, thereby causing a false alarm.
- Antenna characteristics, particularly the two-way antenna pattern sidelobe response, are particularly important with respect to enabling undesired false alarm detections due to clutter.
- Careful design of the system antenna is particularly important to good GMTI/DMTI system performance.
- Tapering the antenna aperture(s) can substantially reduce antenna sidelobes. This might be for the TX pattern, the RX pattern, or both.
- In addition, employing guard antenna(s) to discriminate sidelobe energy can be very useful. Algorithms for such systems are called Sidelobe Cancellers, or Sidelobe Blanking.
- The various detection algorithms have different capabilities with respect to sidelobe clutter. The need for additional processing to deal with clutter after detection will depend on the degree with which sidelobe clutter can be mitigated before detection.

"A child of five would understand this. Send someone to fetch a child of five."
-- Groucho Marx

References

[1] Armin W. Doerry, *Performance Limits for Exo-Clutter Ground Moving Target Indicator (GMTI) Radar*, Sandia National Laboraties Report SAND2010-5844, Unlimited Release, September 2010.

[2] Ann Marie Raynal, Douglas L. Bickel, Michael M. Denton, Wallace J. Bow, Armin W. Doerry, "Radar cross section statistics of ground vehicles at Ku-band," SPIE 2011 Defense & Security Symposium, Radar Sensor Technology XV, Vol. 8021, Orlando FL, 25-29 April 2011.

[3] Ann Marie Raynal, Bryan L. Burns, Tobias J. Verge, Douglas L. Bickel, Ralf Dunkel, Armin W. Doerry, "Radar cross section statistics of dismounts at Ku-band," SPIE 2011 Defense & Security Symposium, Radar Sensor Technology XV, Vol. 8021, Orlando FL, 25-29 April 2011.

[4] A. W. Doerry, D. L. Bickel, A. M. Raynal, "Some comments on performance requirements for DMTI radar," SPIE 2014 Defense & Security Symposium, Radar Sensor Technology XVIII, Vol. 9077, Baltimore MD, 5–9 May 2014.

[5] Maurice W. Long, *Radar Reflectivity of Land and Sea*, ISBN-13: 978-1580531535, Artech House, 1983.

[6] Fawwaz T. Ulaby, M. Craig Dobson, *Radar Scattering Statistics for Terrain*, ISBN-13: 978-0890063361, Artech House, Inc., 1989.

[7] Armin W. Doerry, *Catalog of Window Taper Functions for Sidelobe Control*, Sandia National Laboratories Report SAND2017-4042, Unlimited Release, April 2017.

[8] Ann Marie Raynal, Douglas L. Bickel, Dale F. Dubbert, Tobias J. Verge, Bryan L. Burns, Ralf Dunkel, Armin W. Doerry, "Radar cross section statistics of cultural clutter at Ku-band," SPIE 2012 Defense, Security & Sensing Symposium, Radar Sensor Technology XVI, Vol. 8361, Baltimore MD, 23-27 April 2012.

[9] John P. Stralka, William G Fedarko, "Pulse Doppler Radar", edited by Merrill Skolnik, *Radar Handbook*, Third Edition, ISBN-13: 978-0071485470, McGraw-Hill Education, 2008.

[10] Armin W. Doerry, *Noise and Noise Figure for Radar Receivers*, Sandia National Laboratories Report SAND2016-9649, Unlimited Release, October 2016.

[11] D. L. Bickel, A. W. Doerry, "On minimum detectable velocity," SPIE 2019 Defense & Commercial Sensing Symposium, Radar Sensor Technology XXIII, Vol. 11003, Baltimore, MD, 14-18 April 2019.

[12] Armin W. Doerry, *Catalog of Window Taper Functions for Sidelobe Control*, Sandia National Laboratories Report SAND2017-4042, Unlimited Release, April 2017.

[13] Douglas L. Bickel, *Clutter Locus for Arbitrary Uniform Linear Array Orientation*, Sandia National Laboratories Report SAND2010-8796, Unclassified Unlimited Release, December 2010.

[14] Armin W. Doerry, *Clutter in the GMTI Range-Velocity Map*, Sandia National Laboratories Report SAND2009-1797, Unlimited Release, April 2009.

[15] D. L. Bickel, A. W. Doerry, "On minimum detectable velocity," SPIE 2019 Defense & Commercial Sensing Symposium, Radar Sensor Technology XXIII, Vol. 11003, Baltimore, MD, 14-18 April 2019.

[16] Joseph R. Guerci, *Space-Time Adaptive Processing for Radar*, ISBN-13: 978-1580533775, Artech House Publishers, 2003.

[17] D. Curtis Schleher, *MTI and Pulsed Doppler Radar with MATLAB – second edition*, ISBN-13: 978-1-59693-414-6, Artech House, Inc., 2010.

[18] C. V. Jakowatz Jr., D. E. Wahl, P. H. Eichel, D. C. Ghiglia, P. A. Thompson, *Spotlight-Mode Synthetic Aperture Radar: A Signal Processing Approach*, ISBN 0-7923-9677-4, Kluwer Academic Publishers, 1996.

[19] Armin W. Doerry, Douglas L. Bickel, *GMTI Direction of Arrival Measurements from Multiple Phase Centers*, Sandia National Laboratories Report SAND2015-2310, Unlimited Release, March 2015.

[20] Armin W. Doerry, Douglas L. Bickel, *Single-Axis Three-Beam Amplitude Monopulse Antenna – Signal Processing Issues*, Sandia National Laboratories Report SAND2015-4113, Unlimited Release, May 2015.

[21] Armin W. Doerry, Douglas L. Bickel, *Phase Centers of Subapertures in a Tapered Aperture Array*, Sandia National Laboratories Report SAND2015-9566, Unlimited Release, October 2015.

[22] A. W. Doerry, D. L. Bickel, "Antenna phase center locations in tapered aperture subarrays," SPIE 2016 Defense & Security Symposium, Radar Sensor Technology XX, Vol. 9829, Baltimore, MD, 17-21 April 2016.

[23] A. Farina, "Electronic Counter-Countermeasures", edited by Merrill Skolnik, *Radar Handbook*, Third Edition, ISBN-13: 978-0071485470, McGraw-Hill Education, 2008.

[24] Y. H. Mao, "Rejection of active interference," edited by Gaspare Galati, *Advanced radar techniques and systems*, ISBN: 0-86341-172-X, Peter Peregrinus Ltd. On behalf of Institution of Electrical Engineers, 1993.

[25] H. C. Stankwitz, R. J. Dallaire, J. R. Fienup, "Nonlinear Apodization for Sidelobe Control in SAR Imagery," *IEEE Transactions on Aerospace and Electronic Systems*, Vol. 31, No. 1, pp. 267-279, Jan. 1995.

[26] David F. Crouse, "A crash course in basic single-scan target tracking (abridged)," Proceedings of the SPIE, Radar Sensor Technology XXII, Vol. 10633, Orlando, Florida, USA, 4 May 2018.

[27] David Tahmoush, "Review of micro-Doppler signatures," *IET Radar, Sonar & Navigation*, Vol. 9, No. 9, pp. 1140-1146, December 2015.

[28] Victor C. Chen, David Tahmoush, William J. Miceli, *Radar Micro-Doppler Signatures: Processing and applications*, ISBN-13: 978-1849197168, The Institution of Engineering and Technology, 2014.

[29] David Tahmoush, "Micro-range micro-doppler for dismount classification," Proceedings of the SPIE, Radar Sensor Technology XVII, Vol. 8714, p. 87141E, Baltimore, Maryland, USA, 31 May 2013.

[30] D. L. Bickel, A. W. Doerry, "Measuring channel balance in multi-channel radar receivers," SPIE 2018 Defense & Security Symposium, Radar Sensor Technology XXII, Vol. 10633, Orlando, FL, 15-19 April 2018.

"In fact, when you get right down to it, almost every explanation Man came up with for anything until about 1926 was stupid."
-- Dave Barry

Distribution

Unlimited Release

Hardcopy Internal

1	A. W. Doerry	5349	MS 0519
1	L. Klein	5349	MS 0519
1	M. R. Lewis	5349	MS 0519
1	S. P. Castillo	5340	MS 0532

Email—External

Brandeis Marquette	Brandeis.Marquette@ga-asi.com	General Atomics ASI
Jean Valentine	Jean.Valentine@ga-asi.com	General Atomics ASI
John Fanelle	John.Fanelle@ga-asi.com	General Atomics ASI

Email—Internal

Technical Library	9536	libref@sandia.gov

Sandia National Laboratories is a multimission laboratory managed and operated by National Technology & Engineering Solutions of Sandia LLC, a wholly owned subsidiary of Honeywell International Inc. for the U.S. Department of Energy's National Nuclear Security Administration under contract DE-NA0003525.